



1 **A comparative isotopic study of the biogeochemical cycle of**  
2 **carbon in modern stratified lakes: the hidden role of DOC**

3 Robin Havas<sup>a,\*</sup>, Christophe Thomazo<sup>a,b</sup>, Miguel Iniesto<sup>c</sup>, Didier Jézéquel<sup>d</sup>, David Moreira<sup>c</sup>, Rosaluz Tavera<sup>c</sup>,  
4 Jeanne Caumartin<sup>f</sup>, Elodie Muller<sup>f</sup>, Purificación López-García<sup>c</sup>, Karim Benzerara<sup>f</sup>

5

6 <sup>a</sup> Biogéosciences, CNRS, Université de Bourgogne Franche-Comté, 21 000 Dijon, France

7 <sup>b</sup> Institut Universitaire de France, 75005 Paris, France

8 <sup>c</sup> Ecologie Systématique Evolution, CNRS, Université Paris-Saclay, AgroParisTech, 91190 Gif-sur-Yvette,  
9 France

10 <sup>d</sup> IPGP, CNRS, Université de Paris, 75005 Paris, and UMR CARRTEL, INRAE & USMB, France

11 <sup>e</sup> Departamento de Ecología y Recursos Naturales, Universidad Nacional Autónoma de México, México

12 <sup>f</sup> Sorbonne Université, Muséum National d'Histoire Naturelle, CNRS, Institut de Minéralogie, de Physique des  
13 Matériaux et de Cosmochimie (IMPMC), 75005 Paris, France.

14

15

16 \* Correspondence to: Robin Havas ([robin.havas@gmail.com](mailto:robin.havas@gmail.com))

17

18

19

20

21 *Keywords: Carbon cycle; isotopic fractionation; DOC; Precambrian analogs*

22



23 **Abstract.** The carbon cycle is central to the evolution of biogeochemical processes at the surface of the Earth. In  
24 the ocean, which has been redox-stratified through most of the Earth's history, the dissolved organic carbon (DOC)  
25 reservoir holds a critical role in these processes because of its large size and involvement in many biogeochemical  
26 reactions. However, it is rarely measured and examined in modern stratified analogs and yet commonly invoked  
27 in past C cycle studies. Here, we characterized the C cycles of four redox-stratified alkaline crater lakes from  
28 Mexico. For this purpose, we analyzed the concentrations and isotopic compositions of DOC together with  
29 dissolved inorganic and particulate organic C (DIC and POC). In parallel we measured physico-chemical  
30 parameters of the water columns and surficial bottom sediments. The four lakes have high DOC concentrations  
31 (from ~ 15 to 160 times the amount of POC, averaging  $2 \pm 4$  mM; 1SD, n=28) with an important variability  
32 between and within the lakes. All lakes exhibit prominent DOC peaks (up to 21 mM), found in the oxic and/or  
33 anoxic zones.  $\delta^{13}\text{C}_{\text{DOC}}$  signatures also span a broad range of values from -29.3 to -8.7 ‰ (with as much as 12.5 ‰  
34 variation within a single lake), while  $\delta^{13}\text{C}_{\text{POC}}$  and  $\delta^{13}\text{C}_{\text{DIC}}$  varied from -29.0 to -23.5 ‰ and -4.1 to +2.0 ‰,  
35 respectively. The DOC peaks in the water columns and associated isotopic variability seem mostly related to  
36 oxygenic and/or anoxygenic primary productivity through the release of excess fixed C in three of the lakes  
37 (Atexcac, La Preciosa and La Alberca de los Espinos). By contrast, the variability of [DOC] and  $\delta^{13}\text{C}_{\text{DOC}}$  in Lake  
38 Alchichica could be mainly explained by partial degradation and accumulation in anoxic waters. Overall, DOC  
39 records metabolic reactions that would not have been clearly detected if only DIC and POC reservoirs had been  
40 analyzed. For example, DOC analyses evidence an active DIC-uptake and use of a DIC-concentrating mechanism  
41 by part of the photosynthetic plankton. Despite the prominent role of DOC in the C cycle of these lakes, variations  
42 of [DOC]/ $\delta^{13}\text{C}_{\text{DOC}}$  and associated reactions are not reflected in the sedimentary organic carbon record, hence  
43 calling for special care when considering sediments as reliable archives of metabolic activities in stratified water  
44 columns. Overall, this study brings to light the need of further investigating the role of DOC in the C cycles of  
45 modern stratified analogs.

46

47



## 48 1. INTRODUCTION

49 The carbon cycle and biogeochemical conditions prevailing at the surface of the Earth are intimately bound through  
50 combined biological and geological processes and have evolved together throughout the Earth's history.  
51 Accordingly, the analysis of carbon isotopes from the rock record has been used to reconstruct the evolution of the  
52 biosphere and oxygenation of the Earth's (e.g. Hayes et al., 1989; Karhu and Holland, 1996; Schidlowski, 2001;  
53 Bekker et al., 2008). Because the oceans have been redox-stratified throughout most of the Earth's history (Lyons  
54 et al., 2014; Havig et al., 2015; Satkoski et al., 2015), processes affecting the C cycle were likely different from  
55 those occurring in most modern, well oxygenated environments. This impacts from the diversity and relative  
56 abundance of microbial carbon and energy metabolism (e.g. Paneth and O'Leary, 1985; Hessen and Anderson,  
57 2008; Wang et al., 2016; Iñiguez et al., 2020), to larger ecological interactions (e.g. Jiao et al., 2010; Close and  
58 Henderson, 2020; Klawonn et al., 2021) and global C dynamics (e.g. Ridgwell and Arndt, 2015; Ussiri and Lal,  
59 2017). Nonetheless, some modern stratified analogs (anoxic at depth) of early oceans exist, and need to be  
60 characterized in order to better understand the C cycle in ancient redox-stratified systems and how it was recorded  
61 by the sedimentary archives (e.g. Lehmann et al., 2004; Posth et al., 2017; Fulton et al., 2018). To this end, a  
62 number of recent studies investigated the C cycle of modern stratified water columns (e.g. Crowe et al., 2011;  
63 Kuntz et al., 2015; Camacho et al., 2017; Posth et al., 2017; Schiff et al., 2017; Havig et al., 2018; Cadeau et al.,  
64 2020; Saini et al., 2021; Petrash et al., 2022), with the clear advantage that many of their bio-geo-physico-chemical  
65 parameters could be directly measured, together with the main C reservoirs.

66 Yet, very few studies on redox-stratified analogs included the analysis of dissolved organic carbon (DOC) and  
67 even fewer measured DOC stable isotope data (Havig et al., 2018), despite the fact that it is a major component of  
68 marine and fresh waters (e.g. Ridgwell and Arndt, 2015; Brailsford, 2019). Indeed, DOC generally represents the  
69 majority of freshwater organic matter (Kaplan et al., 2008; Brailsford, 2019), while the size of oceanic DOC equals  
70 the total amount of atmospheric carbon (Jiao et al., 2010; Thornton, 2014). DOC is (i) at the base of many trophic  
71 chains (Bade et al., 2007; Hessen and Anderson, 2008; Jiao et al., 2010; Thornton, 2014), (ii) key in physiological  
72 and ecological equilibria (Hessen and Anderson, 2008) and (iii) has a critical role as a long-term C storage reservoir  
73 for climate change (Jiao et al., 2010; Hansell, 2013; Thornton, 2014; Ridgwell and Arndt, 2015). Although the  
74 contribution of DOC reservoirs to the past and modern Earth's global climate and biogeochemical cycles is not  
75 properly constrained (Jiao et al., 2010; Dittmar, 2015), it has been used to explain some perturbations of the C  
76 cycle recorded in sedimentary archives (e.g. Rothman et al., 2003; Fike et al., 2006; Sexton et al., 2011; Ridgwell  
77 and Arndt, 2015).

78 Here, we propose to describe the C cycle of four modern redox-stratified alkaline crater lakes, located in the trans-  
79 Mexican volcanic belt (Ferrari et al., 2012). They relate to similar geological contexts and climates but have  
80 distinct solution chemistries – aligning along an alkalinity/salinity gradient (Zeyen et al., 2021) – as well as distinct  
81 planktonic communities (Iniesto et al., in press). Moreover, they harbor various types of microbialites (Gérard et  
82 al., 2013; Saghaï et al., 2016; Iniesto et al., 2021a, 2021b; Zeyen et al., 2021). We measured the concentrations  
83 and isotopic compositions of C-containing phases throughout the stratified water column of the lakes, including  
84 DOC, dissolved inorganic carbon (DIC) and particulate organic carbon (POC). In parallel, depth profiles of several  
85 physico-chemical parameters as well as trace and major elements concentrations were measured allowing to  
86 pinpoint the main occurring biogeochemical reactions and connect them with specific C isotopes signatures. Last,



87 surficial sediments (~ 10 cm) at the bottom of the lakes were also characterized in order to further constrain the  
88 main geochemical reactions taking place in the lower water columns and infer possible exchanges between the  
89 sediment and water column reservoirs.

90 Investigations of the C cycle in Precambrian analogs usually focus on a single environment instead of integrating  
91 views from several systems (e.g. Camacho et al., 2017; Schiff et al., 2017). Here, the inter-comparison via the  
92 same methodology of four redox-stratified lakes of the same type (tropical alkaline volcanic crater-lakes) but with  
93 distinct solution chemistries and microbial diversities (Zeyen et al., 2021; Iniesto et al., in press), allows to assess  
94 the effects of specific physico-chemical and biological parameters on the C cycle. Thus, we present the main  
95 biogeochemical reactions occurring in the water columns (e.g. oxygenic/anoxygenic photosynthesis or  
96 methanogenesis) and how they are recorded (or not) in surficial sediments. Then, we shed a new light on the  
97 microbial cycling of DOC and how the analysis of its isotopes can provide deeper insights into microbial processes  
98 and overall C cycle dynamics in stratified water columns. Finally, we discuss the possible implications of DOC  
99 for paleoclimate reconstruction and the interpretation of the sedimentary C isotopes record.

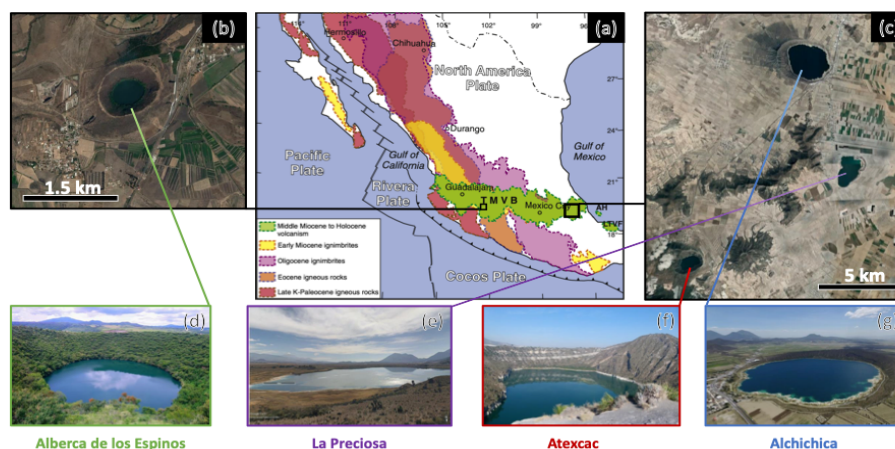
100

## 101 2. SETTING / CONTEXT

### 102 2.1. Geology

103 The four lakes studied here are volcanic maars formed after phreatic, magmatic and phreatomagmatic explosions,  
104 in relation with volcanic activity in the Trans-Mexican-Volcanic Belt (TMVB, Fig. 1). TMVB originates from the  
105 subduction of the Rivera and Cocos plates beneath the North America plate, resulting in a long and wide (~1000  
106 and 90-230 km, respectively) Neogene volcanic arc spreading across central Mexico (Ferrari et al., 2012). The  
107 TMVB harbors a large variety of monogenetic scoria cones and phreatomagmatic vents (maars and tuff-cones) as  
108 well as stratovolcanoes, calderas and domes (Carrasco-Núñez et al., 2007; Ferrari et al., 2012; Siebe et al., 2014).  
109 Maar crater formation usually occurs when ascending magmas meet water-saturated substrates, leading to  
110 successive explosions downward within and excavation of older units (Lorenz, 1986; Carrasco-Núñez et al., 2007;  
111 Siebe et al., 2012; Chako Tchamabé et al., 2020).

112 Three of the studied lakes (Alchichica, Atexcac and La Preciosa) are located in a restricted area (~ 50 km<sup>2</sup>) of the  
113 Serdan-Oriental Basin (SOB) in the easternmost part of the TMVB (Fig. 1). The SOB is a closed intra-montane  
114 basin at high altitude (~2300 m), surrounded by the Los Humeros caldera in the north and Cofre de Perote-  
115 Citlatépel volcanic range in the east. The basement is mainly composed of folded and faulted Cretaceous  
116 limestones and shales, covered by andesitic to basaltic lava flows (Carrasco-Núñez et al., 2007; Armienta et al.,  
117 2008; Chako Tchamabé et al., 2020). The formations of Alchichica and Atexcac craters were dated back to ~ 6-13  
118 ± 5-6 and 330 ± 80 ka, respectively (Table 1; Carrasco-Núñez et al., 2007; Chako Tchamabé et al., 2020). The age  
119 of lake La Preciosa is not known. The fourth lake, La Alberca de los Espinos, is located at the margin of the Zacapu  
120 tectonic lacustrine basin in the Michoacán-Guanajuato Volcanic Field (MGVF) in the western-central part of the  
121 TMVB (Fig. 1). It lies at about 1985 m, mainly on andesitic basement rocks and was dated at ~25 ± 2 ka years  
122 (Siebe et al., 2012, 2014).



123 Figure 1. Geographical location and photographs of the studied crater lakes. (a) Geological map from  
124 Ferrari et al. (2012) representing the location of the four studied lakes in the trans-Mexican volcanic  
125 belt (TMVB). (b), (c) Close up © Google Earth views of lake Alberca de los Espinos and the Serdan-  
126 Oriental Basin (SOB), respectively. (d-g) Pictures of the four studied lakes (d from © Google Image  
127 [‘enamoredemexicowebiste’], e from © Google Earth street view, and g from © ‘Agencia Es Imagen’).  
128

## 129 2.2. Climate and limnology

130 Due to their geographical proximity from each other, lakes from the SOB experience a similar temperate to semi-  
131 arid climate (Armienta et al., 2008; Sigala et al., 2017). The present climate of the SOB is dominated by dry  
132 conditions with evaporation fluxes higher than precipitation fluxes in Lake Alchichica for example (~ 1686 vs  
133 392 mm/an; Alcocer, 2021). In Alchichica, Atexcac and La Preciosa, this trend is reflected by a drop in their water  
134 level evidenced by the emersion of microbialite deposits in these lakes (Fig. S1; Zeyen et al., 2021). This  
135 evaporation-dominated climate strongly contributes to the achievement of relatively high lake salinities from 1.2  
136 to 7.9 psu, ranging from sub- to hyposaline. In comparison, Alberca’s climate is temperate to semi-humid and it is  
137 a freshwater lake (0.6 psu, Rendon-Lopez, 2008; Sigala et al., 2017).

138 The four lakes are warm monomictic, i.e., they are stratified throughout most of the year (~ 9 months) and mix  
139 once a year when the thermal stratification breaks down in the cold winter (Armienta et al., 2008). They are all  
140 “closed lakes” located in an “endorheic” basin (Alcocer, 2021; Zeyen et al., 2021), meaning that they have no  
141 inflow, outflow nor a connection to other basins through surficial waters such as streams. Overall, water input is  
142 only supplied by precipitations, and groundwater inflow as evidenced and quantified for Lake Alchichica (Alcocer,  
143 2021 and references therein).

144 Finally, the four lakes are alkaline (pH ~ 9) but distribute over a gradient of chemical compositions (including  
145 alkalinity, salinity and Mg/Ca ratio) interpreted as reflecting varying concentration stages of an initial alkaline  
146 dilute water (Table 1; Zeyen et al., 2021), evolving due to different climates (mostly between Alberca and lakes



147 from the SOB) and more generally, different hydrological regimes. Microbialite deposits are found in all four lakes  
 148 with an increasing abundance from lower to higher alkaline conditions (Zeyen et al., 2021).

149 Table 1. General information of the studied lakes. Abbreviations: TMVB: Trans-Mexican volcanic  
 150 belt; MGVF: Michoacán-Guanajuato volcanic field; masl: meters above sea level. *NB*: Sampling in  
 151 May 2019 except for La Preciosa's sediments, sampled in May 2016.

Lake	General location	Sampling location	Elevation
Alchichica	Serdan Oriental Basin, eastern TMVB	19°24'51.5" N; 097°24'09.9" W	2320
Atexcac	Serdan Oriental Basin, eastern TMVB	19°20'2.2" N; 097°26'59.3" W	2360
La Preciosa	Serdan Oriental Basin, eastern TMVB	19°22'18.1" N; 097°23'14.4" W	2330
La Alberca de los Espinos	Zacapu Basin, MGVF, central TMVB	19°54'23.9" N; 101°46'07.8" W	1985

152

Lake	Lake Basement	Age	Max Depth (m)	Alkalinity (mmoles/L)	Salinity (psu)	pH
Alchichica	limestone, basalts	6-13 ± 5-6 ka	63	~35	7.9	9.22
Atexcac	limestone, andesites, basalts	330 ± 80 ka	39	~26	7.4	8.85
La Preciosa	limestone, basalts	Pleistocene	46	~13.5	1.15	9.01
La Alberca de los Espinos	andesite xenoliths	25 ± 2 ka	30	~7	0.6	9.14

153

154

### 155 3. METHOD

#### 156 3.1. Sample Collection

157 The sediment core from Lake La Preciosa was collected in May 2016. All other samples were collected in May  
 158 2019. The depth profiles of several physico-chemical parameters were measured in the water columns of the four  
 159 lakes using an YSI Exo 2 multi-parameter probe: temperature, pH, ORP, conductivity, O<sub>2</sub>, chlorophyll a,  
 160 phycocyanin, and turbidity. Precisions for these measurements were 0.01 °C, 0.1 pH unit, 20 mV, 0.001 mS/cm,  
 161 0.1 mg/L, 0.01 µg/L, 0.01 µg/L and 2% FNU unit, respectively. The ORP signal was semi-calibrated and was used  
 162 to report relative variations over a depth profile. Measurements of the aforementioned parameters allowed to  
 163 pinpoint depths of interest for further chemical and isotopic analyses, notably around the chemoclines of the lakes.  
 164 Water samples were collected with a Niskin bottle. For analyses of dissolved inorganic and organic carbon (DIC,  
 165 DOC), major, minor and trace ions, between 1.5 and 5 L of lake water were filtered at 0.22 µm with Filtropur S  
 166 filters that were pre-rinsed with the lake water. Particulate matter was collected on pre-ashed and weighted glass  
 167 fiber filters (Whatman GF/F, 0.7 µm) and analyzed for particulate organic carbon (POC), major and trace elements.



168 Sediment cores were collected using a 90 mm Uwitec corer at the bottom of each lake's where the water column  
169 was at its deepest (Table 1) and anoxic conditions prevail almost all year long. Cores measured between 20 and  
170 85 cm in length. Slices of about 2-3 cm were cut. Interstitial pore water was drained out of the core slices using  
171 Rhizons. Sediments were then fully dried in a laboratory anoxic N<sub>2</sub>-filled glove box.

172

### 173 **3.2. Dissolved inorganic carbon (DIC) concentration and isotope measurements**

174 Twelve milliliters of 0.22- $\mu$ m-filtered solutions were placed in hermetic Exetainer® tubes in order to avoid  
175 exchange between DIC and atmospheric CO<sub>2</sub>. DIC concentrations and isotopic compositions were determined at  
176 the Institut de Physique du Globe de Paris (IPGP), using an Analytical Precision 2003 GC-IRMS, running under  
177 He-continuous flow, and following the protocol described by Assayag et al. (2006). In short, a given volume of  
178 water sample is taken out of the Exetainer® tube with a syringe, while the same volume of helium is introduced  
179 in order to maintain a stable pressure and atmospheric-CO<sub>2</sub>-free conditions within the sample tubes. The collected  
180 sample is introduced in another Exetainer® tube that was pre-filled with a few drops of 100% phosphoric acid  
181 (H<sub>3</sub>PO<sub>4</sub>) and pre-flushed with He gas. Under acidic conditions, the DIC quantitatively converts to gaseous and  
182 aqueous CO<sub>2</sub>, which equilibrates overnight within the He filled head space of the tube. Quantification and isotopic  
183 analyses of released gaseous CO<sub>2</sub> are then carried out by GC-IRMS using internal standards of known composition  
184 that were prepared and analyzed via the same protocol. Each measurement represents an average of four injections  
185 in the mass spectrometer. Chemical preparation and IRMS analysis were duplicated for all the samples. The  $\delta^{13}\text{C}_{\text{DIC}}$   
186 reproducibility calculated for the 65 samples was better than  $\pm 0.2$  ‰, including internal and external  
187 reproducibility. Standard deviation for [DIC] was  $0.6 \pm 0.9$  mmol/L on average.

188 Specific DIC speciation, i.e., CO<sub>2(aq)</sub>, HCO<sub>3</sub><sup>-</sup> and CO<sub>3</sub><sup>2-</sup> activities, was computed using Phreeqc with the full  
189 dissolved chemical composition of each sample as an input. It should be noted that these results are provided by  
190 calculations of theoretical chemical equilibria and do not necessarily take into account local kinetic effects, which,  
191 for example, could lead to local exhaustion of CO<sub>2(aq)</sub> where intense photosynthesis occurs. Additionally, dating  
192 of the DIC was achieved by measuring its <sup>14</sup>C content and was performed by Beta Analytic laboratory, Miami,  
193 USA.

194

### 195 **3.3. Dissolved organic carbon (DOC) concentrations and isotope measurements**

196 Samples of filtered solutions were first acidified to a pH of about 1-2 in order to degas all the DIC and preserve  
197 the DOC only. DOC concentrations were measured with a Vario TOC at the Biogéosciences Laboratory calibrated  
198 with a range of potassium hydrogen phthalate (Acros®) solutions. Before isotopic analyses, DOC concentration  
199 of the samples was adjusted to match our international standards at 5 ppm (USGS 40 glutamic acid and USGS 62  
200 caffeine). Isotopic compositions were measured at the Biogéosciences Laboratory using an IsoTOC (running under  
201 He-continuous flow) coupled with an IsoPrime stable isotope ratio mass spectrometer (IRMS; IsoPrime,  
202 Manchester, UK). Samples were stirred with a magnetic bar and flushed with He before injection of 1 mL sample  
203 aliquots (repeated 3 times). DOC is then transformed into gaseous CO<sub>2</sub> by combustion at about 850 °C,  
204 quantitatively oxidized by copper oxides and separated from other combustion products in a reduction column and



205 water condensers. Finally, it is transferred to the IRMS via an open split device. In order to avoid a significant  
206 memory effect between consecutive analyses, samples were separated by six aliquots of deionized water and their  
207 first aliquot was discarded from the isotopic calculations. Average reproducibility of  $\delta^{13}\text{C}_{\text{DOC}}$  on standards and  
208 samples was 1 and 0.5 ‰ (1SD), respectively. Average reproducibility for sample [DOC] measurements was on  
209 average 0.3 mM.

210

#### 211 **3.4. Particulate organic carbon and nitrogen (POC / PON)**

212 Particulate organic matter from the lakes water columns was collected on GF/F quartz filters, ground in a ball mill  
213 before and after decarbonation. Decarbonation was performed with 12N HCl vapors in a desiccator for 48 h.  
214 Aliquots of dry decarbonated samples (25 - 70 mg) were weighed in tin capsules. POC and PON contents and  
215  $\delta^{13}\text{C}_{\text{POC}}$  were determined at the Biogéosciences Laboratory using a Vario MICRO cube elemental analyzer  
216 (Elementar, Hanau, Germany) coupled in continuous flow mode with an IsoPrime IRMS (Isoprime, Manchester,  
217 UK). USGS 40 and IAEA 600 certified materials were used for calibration and showed a reproducibility better  
218 than 0.15 ‰ for  $\delta^{13}\text{C}$ . External reproducibility based on triplicate analyses of samples (n=23) was 0.1 ‰ on average  
219 for  $\delta^{13}\text{C}_{\text{POC}}$  (1SD). External reproducibilities of POC and PON concentrations were on average 0.001 and  
220 0.005 mmol/L, respectively (i.e. 3 and 7 % of measured concentrations).

221

#### 222 **3.5. Geochemical characterizations of the sediments**

223 Sedimentary organic carbon (SOC), sedimentary organic nitrogen (SON) and their isotopic compositions were  
224 measured on carbonate-free residues of the first 12 cm of sediments, produced after overnight 1N HCl digestion.  
225 Plant debris (mainly found in La Alberca and Atexcac) were picked upon initial sediment grinding in an agate  
226 mortar and analyzed separately. Aliquots of dried decarbonated samples (~4-70 mg) were weighed in tin capsules.  
227 SOC and SON contents and  $\delta^{13}\text{C}$  were determined at the Biogéosciences Laboratory using a Vario MICRO cube  
228 elemental analyzer (Elementar GmbH, Hanau, Germany) coupled in continuous flow mode with an IsoPrime  
229 IRMS (Isoprime, Manchester, UK). USGS 40 and IAEA 600 certified materials were used for calibration and had  
230 reproducibility better than 0.2 ‰ for  $\delta^{13}\text{C}_{\text{SOC}}$ . Sample analyses (n=67) were at least duplicated and showed an  
231 average external reproducibility of 0.1 ‰ for  $\delta^{13}\text{C}$  (1SD). External reproducibilities for SOC and SON contents  
232 were 0.1 and 0.03 wt. %, respectively.

233 Carbon isotopic compositions of carbonates from the bottom sediments in La Alberca were analyzed at the  
234 Biogéosciences Laboratory using a ThermoScientific™ Delta V Plus™ IRMS coupled with a Kiel VI carbonate  
235 preparation device. External reproducibility was assessed by multiple measurements of NBS19 standard and was  
236 better than  $\pm 0.1$  ‰ ( $2\sigma$ ).

237 Solid sulfides minerals concentrations were determined on dry bulk sediments in Lake La Alberca after a wet  
238 chemical extraction using a boiling acidic Cr(II)-solution as detailed in Gröger et al. (2009).

239

#### 240 **3.6. Major and trace elements concentrations**



241 Dissolved and particulate matter elemental compositions were measured at the Pôle Spectrométrie Océan  
 242 (Plouzané, France) by inductively coupled plasma atomic-mass spectroscopy (ICP-AES, Horiba Jobin) for major  
 243 elements and by high resolution-ICP-mass spectrometry using an Element XR (HR-ICP-MS, Thermo Fisher  
 244 Scientific) for trace elements. Major element measurement reproducibility based on internal multi-elemental  
 245 solution was better than 5%. Trace elements were analyzed by a standard-sample bracketing method and calibrated  
 246 with a multi-elemental solution. Analytical precision for trace elements was generally better than 5%. Dissolved  
 247 sulfates/chloride and ammonium concentrations ( $\text{NH}_4^+$ ) were determined at the IPGP by chromatography and by  
 248 continuous flow colorimetric analysis, respectively, with an uncertainty lower than 5%.

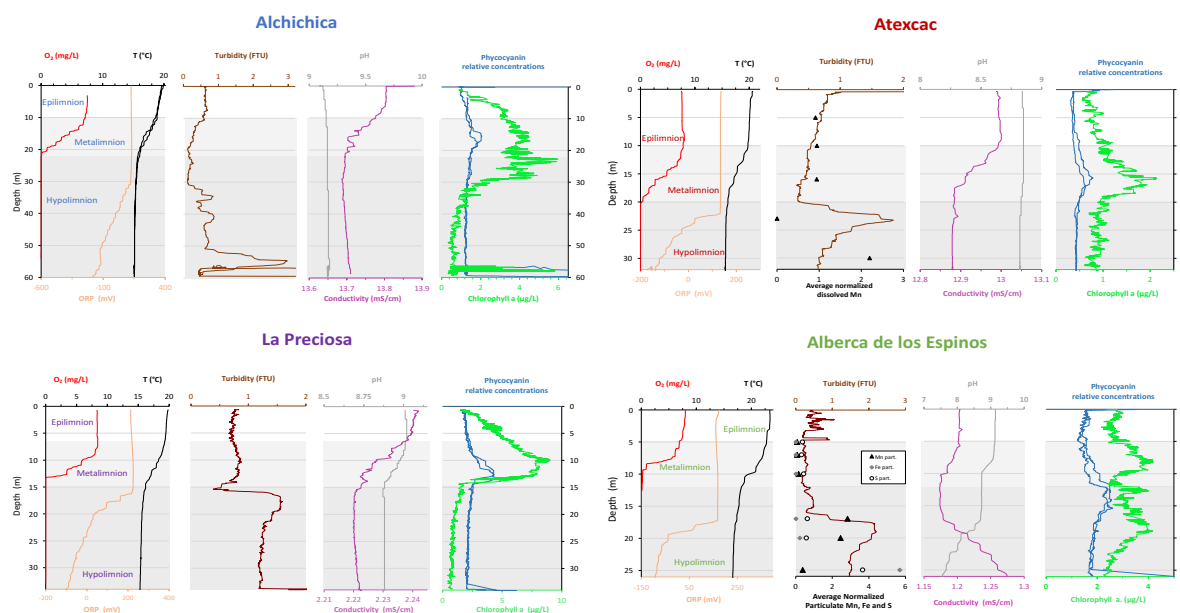


Figure 2. Physico-chemical parameters depth profiles of Alchichica, Atexcac, La Preciosa and Alberca de los Espinos including: dissolved oxygen concentrations (mg/L), water temperature ( $^{\circ}\text{C}$ ), oxidation-reduction potential (ORP, mV), turbidity (Formazin Turbidity Unit), pH, conductivity (mS/cm), phycocyanin and chlorophyll a. pigments ( $\mu\text{g/L}$ ). Absolute values for phycocyanin concentrations were not determined; only relative variations are represented (with increasing concentrations to the right). Discrete concentration values of dissolved Mn in Atexcac and particulate Mn, Fe and S in Alberca, normalized by their respective average were added. Epi-, meta- and hypo-limnion layers are represented for each lake according to  $\text{O}_2$  and temperature profiles.

249

## 250 4. RESULTS

251

### 252 4.1. Lake Alchichica

253 The water column of Lake Alchichica showed a pronounced stratification compared to previous years at the same  
 254 period (Fig. 2, Fig. S2; Lugo et al., 2000; Adame et al., 2008; Macek et al., 2020). The water temperature varied  
 255 from about  $20^{\circ}\text{C}$  at the surface to  $15.5^{\circ}\text{C}$  at a 30 m depth and below. Conductivity slightly decreased from 13.8  
 256 to  $13.7\text{ mS/cm}$  between the surface and 20 m in depth (salinity decreasing from 7.9 to 7.8 psu). Dissolved  $\text{O}_2$  was  
 257 saturated at the lake surface (112 % or  $7.5\text{ mg/L}$ ) and rapidly decreased to  $0\text{ mg/L}$  between  $\sim 10$  and 20 m in depth.



258 The oxidation reduction potential (ORP) signal was stable between 130 and 120 mV from the surface to 30 m and  
259 then decreased down to -270 mV at 60 m of depth. Chlorophyll a averaged 2  $\mu\text{g/L}$ , with a broad peak between ~  
260 7 and 29 m at around 4  $\mu\text{g/L}$  (with a 6  $\mu\text{g/L}$  maximum at 23 m) and then decreased to minimum values (0.5  $\mu\text{g/L}$ )  
261 in the lower water column. Finally, pH remained constant at ~9.2 over the whole water column. Based on these  
262 results, the epi-, meta- and hypolimnion layers of Lake Alchichica in May 2019 extended from 0-10, 10-20 and  
263 20-60 m, respectively (Fig. 2).

264 Dissolved inorganic carbon (DIC) represented about 95% of all the carbon (DIC+DOC+POC) in the pelagic water  
265 column. Its concentration was almost constant between 34.5 and 35 mM throughout the whole water column except  
266 at 10 m where it significantly decreased to 33 mM (Fig. 3, Table 2). The  $\delta^{13}\text{C}_{\text{DIC}}$  decreased from 2 to ~ 1.5‰  
267 between 5 and 60 m in depth (Fig. 4). The analysis of  $\text{D}^{14}\text{C}$  content at a depth of 35 m reached 39 % modern  
268 carbon (pMC), equivalent to an apparent age of ~ 7540 years before “present” (i.e. before 1950). Particulate  
269 organic carbon (POC) represented about 0.13 % of the total carbon measured in the water column with a  
270 concentration of 0.07 mM at a 5 m depth, increasing to a maximum of 0.1 mM at 30 m and then decreasing to  
271 ~0.02 mM in the bottom part of the water column. The C:N ratio of particulate organic matter (POM) showed a  
272 similar profile with values around 10.5 down to 30 m, progressively decreasing towards 5.9 at 55 m (Fig. 3).  
273  $\delta^{13}\text{C}_{\text{POC}}$  increased from -26.5 ‰ in the top 30 meters to -24.1 ‰ at 55 m in depth. Dissolved organic carbon (DOC)  
274 represented about 5% of total carbon, with concentrations around 0.5 mM throughout the water column except in  
275 the hypolimnion where it reached up to 5.4 mM. Its isotopic composition varied from -29.3 to -25.1 ‰, with  
276 maximum values found in the hypolimnion (Fig. 4).

277 The sum and weighted average of total carbon concentrations and isotopic compositions were calculated. The total  
278 carbon concentration depth profile roughly follows that of DOC, while  $\delta^{13}\text{C}_{\text{total}}$  is roughly comprised between 2  
279 and 0 ‰ through the water column, except in the lower part of the hypolimnion where it decreases down to -2.4 ‰  
280 on average (Figs. 3, 4; Table 2).

281 Total dissolved phosphorus (TDP) is stable down to 20 m where it shows a marked increase from 0.37 to 1.56  $\mu\text{M}$   
282 at 30 m and then progressively increases up to 3.20  $\mu\text{M}$  at the bottom of the lake (Fig. 5, Table S1). Sulfate  
283 concentration slightly decreases from ~11.8 to 11.7 mM between the surface and 30 m and then increases to  
284 12.2 mM at 60 m. Dissolved Cl followed a similar profile with values around 107 mM at the surface decreasing  
285 below 106 mM at 30 m and increasing back to 111 mM at 60 m (Table S1). Dissolved Mn surprisingly showed  
286 the highest concentrations near the surface (~1.6  $\mu\text{M}$ ) before decreasing to ~0.4  $\mu\text{M}$  between 20 and 55 m and  
287 increasing to 1  $\mu\text{M}$  at 60 m. Similarly, dissolved Fe was higher at the lake surface (~0.3  $\mu\text{M}$ ) and progressively  
288 decreased near 0 at 50/55m (Fig. 5, Table S1).

289 In the first 12 cm of sediments, porewater DIC had concentrations (~ 35 mM) and  $\delta^{13}\text{C}_{\text{DIC}}$  (~ 0 ‰) similar to and  
290 slightly lower than the water column values, respectively. Sedimentary organic matter had a  $\delta^{13}\text{C}_{\text{SOC}}$  increasing  
291 from -25.7 to -24.5 ‰ and C:N ratios slightly higher than 10 (Figs. 3, 4; Table S2).

#### 292 293 **4.2. Lake Atexcac**

294 Stratification of the Lake Atexcac water column was also very well defined (Fig. 2). Temperature was high (20.6  
295 – 19.6 °C) between 0 and 10 m in depth; it rapidly decreased and remained constant at 16 °C below 20 m.



296 Conductivity had the same evolution with values around 13 mS/cm near the surface and decreasing to 12.9 mS/cm  
 297 under 20 m (salinity decreasing from about 7.44 to 7.3 psu). Dissolved O<sub>2</sub> was saturated at the lake surface (115 %,   
 298 i.e., 7.6 mg/L) and rapidly decreased to 0 mg/L between ~ 10 and 20 m. The ORP signal was almost constant (~   
 299 134 mV) between the surface and 22 m in depth, before decreasing and reaching -175 mV at a 32 m depth.   
 300 Chlorophyll a averaged 1 µg/L and showed a narrow peak centered at around 16 m reaching ~2 µg/L, with similar   
 301 values at the surface and bottom of the lake (0.8 µg/L). Turbidity showed a pronounced increase below 20 m,   
 302 peaking at 23.3 m and returning to surface values at 26 m. Finally, pH remained between 8.80 and 8.85 throughout   
 303 the water column. Based on these results, the epi-, meta- and hypolimnion of Atexcac in May 2019 can be broadly   
 304 defined as extending from 0-10, 10-20 and 20-39 m, respectively (Fig. 2).

305 DIC represented about 84 % of all carbon present (DIC+DOC+POC) in the pelagic water column. Its concentration   
 306 remained around 26.5 mM from the surface down to 16 m in depth. Below 16 m, DIC decreased in the   
 307 hypolimnion, and notably at 23 m where it reached a value of 24.2 mM (Fig. 3, Table 2). The δ<sup>13</sup>C<sub>DIC</sub> was stable   
 308 around 0.4 ‰ in the epi-/metalimnion. It markedly increased to 0.9 ‰ at 23 m and reached minimum values   
 309 (0.2 ‰) at the bottom of the lake. POC represented about 0.13 % of the total carbon measured in the water column   
 310 with concentrations of 0.05 mM in the epi- and metalimnion, decreasing to 0.02 mM in the hypolimnion. The C:N   
 311 ratio of POM showed the same depth profile as POC concentration with a value around 9.6 in the epi-/metalimnion   
 312 decreasing to 6.6 in the hypolimnion (Fig. 3). δ<sup>13</sup>C<sub>POC</sub> had values around -28.3 ‰ in the epilimnion, showed a   
 313 minimum value of -29 ‰ at 16 m and increased to -26.5 ‰ in the hypolimnion. DOC represented about 16% of   
 314 total carbon, with a concentration around 1.1 mM throughout the water column except at 16 and 23 m, where it

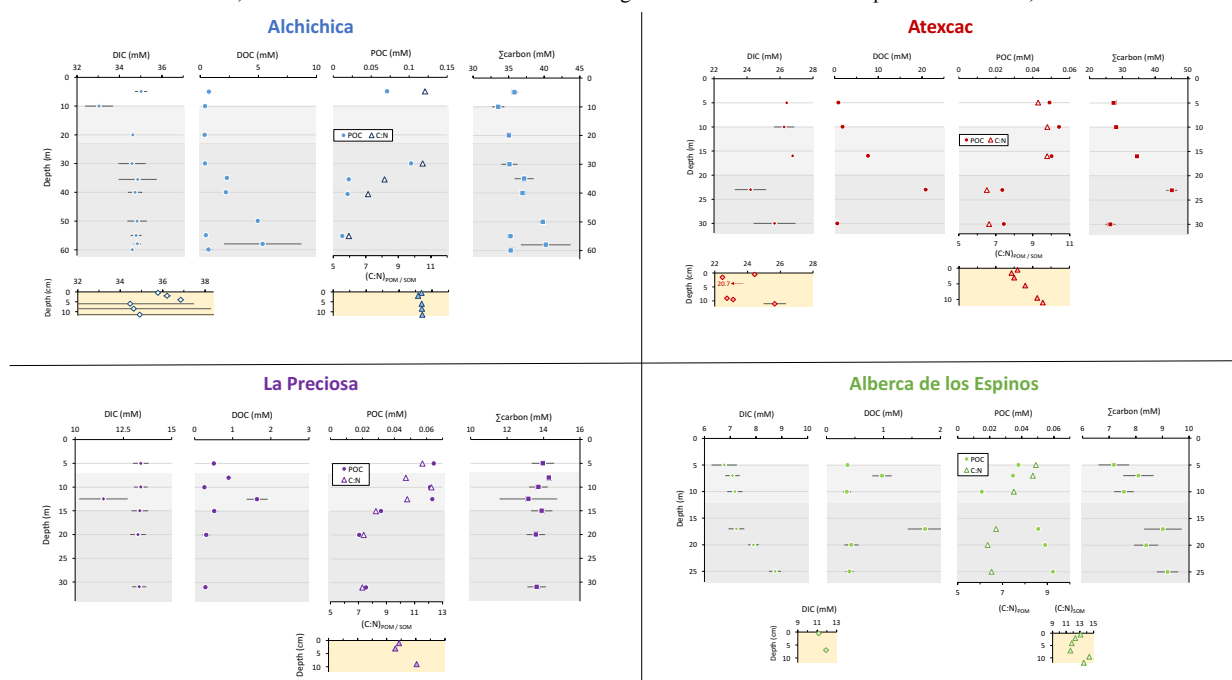


Figure 3. Concentrations in mmoles/L of DIC, DOC, POC and sum of all three reservoirs, C:N molar ratios of POM as a function of depth in the water columns, as well as DIC concentrations in the surficial sediment porewaters and C:N molar ratios of sedimentary OM. Porewaters from La Preciosa's 2016 core were not retrieved.



315 reached 7.7 and 20.8 mM, respectively. Its isotopic composition showed values increasing from -20 to -9 ‰  
 316 between 5 and 23 m, and decreasing to -11 ‰ at 30 m. Total C concentrations and  $\delta^{13}\text{C}_{\text{total}}$  are centered around  
 317 27.7 mM and -0.6 ‰ with a clear increase to 38.9 mM and decrease to -2.7 ‰ at 23 m, respectively.

318 TDP concentrations slightly decreased from ~0.25  $\mu\text{M}$  to 0.19  $\mu\text{M}$  at 16 m, then increased in the hypolimnion to  
 319 ~0.45  $\mu\text{M}$  (Fig. 5; Table S1). Dissolved sulfate concentration was relatively stable at around 2.51 mM throughout  
 320 the water column except at 23 m, where it increased to 2.64 mM. Dissolved Cl concentration slightly decreased  
 321 from 122 to 121 mM between the surface and 16 m before increasing in the hypolimnion at ~125 mM (Table S1).  
 322 Dissolved Mn concentration was constant at 1  $\mu\text{M}$  down to 16 m before dropping to 0 at 23 m and then increasing  
 323 again to a maximum value of 2.35  $\mu\text{M}$  at 30 m (Fig. 5; Table S1). This type of profile evolution was also found  
 324 for other heavy elements such as Cu, Sr, Ba or Pb among others.

325 In the first 12 cm of sediments, porewater DIC concentration varied between ~21 and 26 mM and  $\delta^{13}\text{C}_{\text{DIC}}$  was  
 326 around 0 ‰. Sedimentary organic matter had a  $\delta^{13}\text{C}_{\text{SOC}}$  around -27 ‰ and a C:N ratio increasing from 8 to 10  
 327 (Figs. 3, 4; Table S2).

Table 2  
 Concentrations and isotopic compositions for dissolved inorganic and organic carbon (DIC, DOC), particulate organic carbon (POC) and C:N molar ratios of  
 particulate organic matter (POM). Total carbon concentrations is the sum of all carbon reservoirs measured,  $\delta^{13}\text{C}_{\text{Total}}$  is the weighted average of each  $\delta^{13}\text{C}$ .

Lake	Sample	DIC	DOC	POC	Total Carbon	(C:N) <sub>POM</sub>	$\delta^{13}\text{C}_{\text{DIC}}$	$\delta^{13}\text{C}_{\text{POC}}$	$\delta^{13}\text{C}_{\text{DOC}}$	$\delta^{13}\text{C}_{\text{Total}}$
		mmoles/L				(molar)	‰			
Alchichica	AL 5m	35.0	0.7	0.07	35.8	10.6	2.0	-26.7		1.4
	AL 10m	33.0	0.4		33.5		2.0		-28.3	1.6
	AL 20m	34.6	0.4		35.0		1.6		-29.3	1.3
	AL 30m	34.6	0.4	0.10	35.1	10.5	1.7	-26.3	-28.3	1.2
	AL 35m	34.9	2.3	0.02	37.2	8.1	1.6	-25.7	-26.8	-0.2
	AL 40m	34.7	2.2	0.02	37.0	7.1	1.6	-25.1	-25.8	-0.1
	AL 50m	34.8	5.0		39.8		1.6		-25.1	-1.8
	AL 55m	34.8	0.5	0.01	35.3	5.9	1.5	-24.1	-27.6	1.1
	AL 58m	34.8	5.4		40.2		1.6		-27.7	-2.3
	AL 60m	34.6	0.7		35.3		1.5		-26.1	1.0
Atexcac	ATX 5m	26.4	0.92	0.05	27.4	9.3	0.4	-28.4	-20.0	-0.4
	ATX 10m	26.2	1.8	0.05	28.1	9.8	0.4	-28.2	-15.5	-0.7
	ATX 16m	26.8	7.8	0.05	34.7	9.8	0.3	-29.0		0.2
	ATX 23m	24.2	21.0	0.02	45.2	6.5	0.9	-26.7	-8.7	-3.6
	ATX 30m	25.7	0.7	0.02	26.4	6.6	0.2	-26.4	-11.2	-0.1
La Preciosa	LP 5m	13.4	0.5	0.06	14.0	11.6	0.1	-26.4	-27.2	-0.9
	LP 8m		0.9	0.07		10.4		-27.1	-20.0	
	LP 10m	13.4	0.3	0.06	13.7	12.2	0.2	-27.4	-15.5	-0.4
	LP 12.5m	11.5	1.6	0.06	13.2	10.5	-0.2	-27.1		-2.8
	LP 15m	13.4	0.5	0.03	13.9	8.2	-0.3	-23.5	-8.7	-1.3
	LP 20m	13.3	0.3	0.02	13.6	7.4	-0.4	-26.3	-11.2	-1.0
	LP 31m	13.3	0.3	0.02	13.6	7.3	-0.4	-25.2	-25.4	-0.9
Alberca de Los Espinos	Albbsp 5m	6.8	0.4	0.04	7.2	8.5	-2.6	-27.0	-26.7	-3.9
	Albbsp 7m	7.1	1.0	0.03	8.1	8.3	-2.3	-26.2	-14.7	-3.9
	Albbsp 10m	7.2	0.4	0.02	7.6	7.5	-4.1	-28.3	-25.2	-5.1
	Albbsp 17m	7.2	1.7	0.05	9.0	6.7	-3.4	-29.0	-26.3	-7.9
	Albbsp 20m	7.9	0.4	0.05	8.4	6.3	-3.3	-26.5	-25.1	-4.5
	Albbsp 25m	8.7	0.4	0.06	9.2	6.5	-2.0	-25.7	-27.2	-3.2

328

### 329 4.3. Lake La Preciosa

330 Lake La Preciosa was also stratified (Fig. 2). The temperature varied from about 20 °C at the surface to 16°C at  
 331 15 m. Conductivity had a similar evolution decreasing from 2.24 to 2.22 mS/cm between the surface and 15 m  
 332 (salinity decreasing from 1.15 to 1.14 psu). Dissolved O<sub>2</sub> was saturated at the lake surface (120 %, i.e., 8.4 mg/L)  
 333 and rapidly decreased to 0 between ~8 and 14 m. The ORP signal was stable between 213 and 225 mV from the

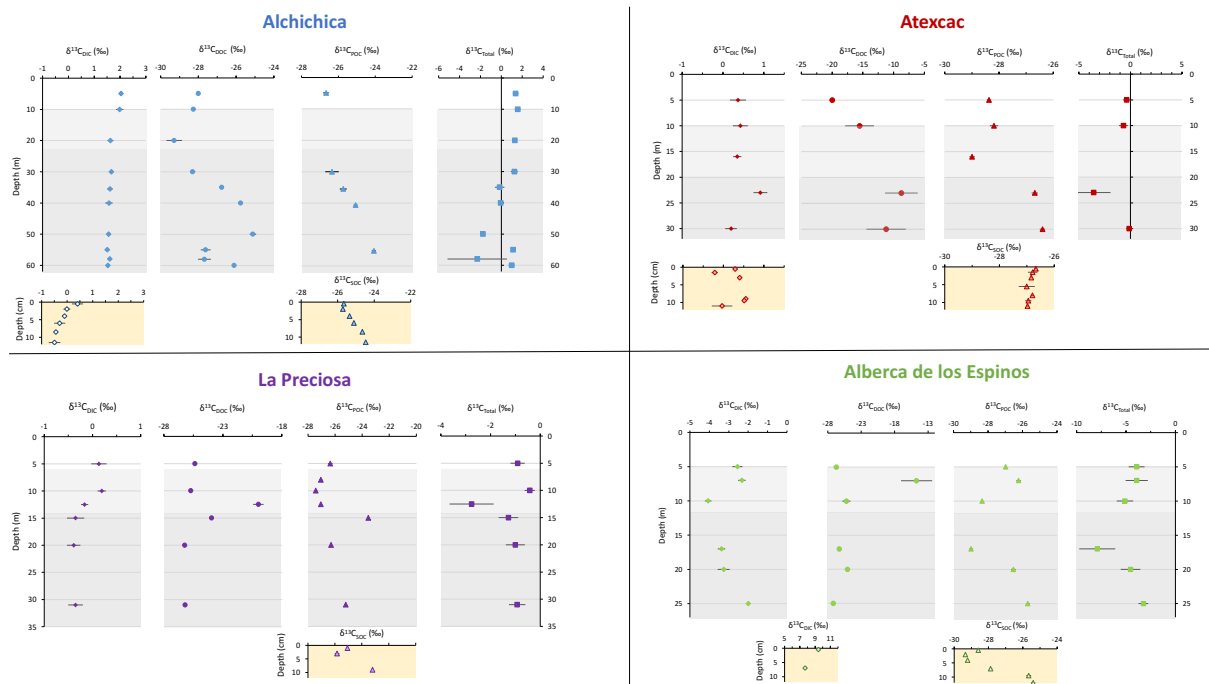


Figure 4. Isotopic compositions of DIC, DOC, POC and weighted average of all three C reservoirs as a function of depth in the water columns as well as isotopic compositions of the porewater-DIC and solid organic carbon from the surficial sediments.

334 lake surface to 16 m and then decreased down to -105 mV at a 35 m depth. Chlorophyll a concentration averaged  
 335 3  $\mu\text{g/L}$  in Lake La Preciosa water column and recorded the highest peak compared to the other lakes, increasing  
 336 to about 9  $\mu\text{g/L}$  at 10 m and decreasing below 12 m to reach minimum values (0.7  $\mu\text{g/L}$ ) below 15 m. Turbidity  
 337 showed a bimodal profile with low values between 0 and 15 m, a large peak between 16 and 19 m and relatively  
 338 high values downward. Finally, pH showed a small decrease from 9 to 8.8 between the surface and 15 m. Based  
 339 on these results, epi-, meta- and hypolimnion layers of La Preciosa in May 2019 can be broadly defined as  
 340 extending from 0-6, 6-15 and 15-45m, respectively (Fig. 2).

341 DIC represented about 97% of all carbon present (DIC+DOC+POC) in La Preciosa water column. Its concentration  
 342 was constant throughout the water column at 13.3 mM, with an exception at 12.5 m, where DIC decreased to  
 343 11.5 mM (Fig. 3, Table 2). The  $\delta^{13}\text{C}_{\text{DIC}}$  decreased from about 0.5 ‰ to -0.36 ‰ between the surface and the  
 344 hypolimnion. POC represented about 0.3% of the total carbon measured in the water column with a concentration  
 345 of 0.06 mM in the epi- and metalimnion, decreasing to 0.02 mM in the hypolimnion. The C:N ratio of POM showed  
 346 a very similar depth profile with a value around 11.2 in the epi-/metalimnion decreasing to 7.6 in the hypolimnion.  
 347  $\delta^{13}\text{C}_{\text{POC}}$  decreased from -26.4 to -27.4 ‰ between 5 and 10 m and peaked at -23.5 ‰ at 15 m before returning to  
 348 value close to -25 ‰ downward. DOC represented about 3% of the total carbon, with a concentration around  
 349 0.5 mM throughout the water column except at 15 m where it peaked at 1.6 mM.  $\delta^{13}\text{C}_{\text{DOC}}$  was mostly around -26  
 350 ‰ except between 10 and 12.5 m, where it reached up to -20 ‰. The total C concentration was relatively stable  
 351 at  $\sim 13.8$  mM, while  $\delta^{13}\text{C}_{\text{total}}$  was centered around -1 ‰ with a decrease down to -2.8 ‰ at 12.5 m.



352 TDP was stable at  $\sim 0.21 \mu\text{M}$  between 5 and 12.5 m and increased in the hypolimnion to  $0.31 \mu\text{M}$  (Fig. 5, Table  
353 S1). Dissolved sulfate concentration slightly decreased from  $\sim 1.22$  to  $1.15 \text{ mM}$  between the surface and 12.5 m  
354 and was stable at  $\sim 1.16 \text{ mM}$  downward. The total S concentration remained stable throughout the water column at  
355 a value of  $\sim 1.19 \text{ mM}$ . Dissolved Cl followed a similar profile with a value around  $8.4 \text{ mM}$  at the surface decreasing  
356 to  $\sim 7.8 \text{ mM}$  below 12.5 m (Table S1). Dissolved Mn was around  $1 \mu\text{M}$  at 5 m, decreased to  $0.3$  and  $0.6 \mu\text{M}$   
357 between 8 and 15 m and increased back to values above  $1 \mu\text{M}$  below that. Dissolved Fe was above detection limit  
358 ( $\sim 0.1 \mu\text{M}$ ) at a 5 m depth ( $0.12 \mu\text{M}$ ) only (Fig. 5; Table S1).

359 In the first 10 cm of the sediments,  $\delta^{13}\text{C}_{\text{SOC}}$  values increased downwards from  $\sim -25.5$  to  $-23.2 \text{ ‰}$  and C:N ratios  
360 from 9.8 to 11 (Figs. 3, 4; Table S2). Porewaters from the 2016 core were not retrieved.

361

#### 362 4.4. Lake La Alberca de los Espinos

363 Stratification of the water column in La Alberca de los Espinos was also well defined (Fig. 2). Temperature was  
364 around  $23 \text{ }^\circ\text{C}$  between 0 and 5 m in depth; it rapidly decreased to  $18.2 \text{ }^\circ\text{C}$  at 12 m and slowly decreased down to  
365  $16.5 \text{ }^\circ\text{C}$  at 26 m. Conductivity was at  $1.20 \text{ mS/cm}$  down to 6 m, and decreased to  $1.17 \text{ mS/cm}$  down to 16 m before  
366 increasing to  $1.27 \text{ mS/cm}$  at 26 m (salinity between 0.58 and 0.64 psu). Dissolved  $\text{O}_2$  was saturated at the lake  
367 surface (118 %, i.e.,  $7.9 \text{ mg/L}$ ) and rapidly decreased to 0 between  $\sim 5$  and 12 m. The ORP signal was mostly  
368 comprised between 160 and 170 mV between the surface and 17 m before decreasing to  $-65 \text{ mV}$  at 21 m and  $-92$   
369  $\text{mV}$  at 26 m. La Alberca had relatively high chlorophyll a levels throughout the water column ( $3.1 \mu\text{g/L}$  on  
370 average) but showed at least three distinctive peaks, all reaching approximately  $4 \mu\text{g/L}$ . They were found (i)  
371 between 6 and 9.5 m, (ii) at around 12.5 m and (iii) between 16 and 19 m. The turbidity profile showed a  
372 pronounced increase from 16 to 19 m, and a slight decrease towards the sediment-water interface. The pH showed  
373 relatively important variations from 9.15 at the lake surface to 8.75 between 6.5 and 10 m, further decreasing to  
374 7.5 between 16 and 26 m. Based on these results, epi-, meta- and hypolimnion layers of Lake La Alberca de los  
375 Espinos in May 2019 can be defined as extending from 0-5, 5-12 and 12-30 m, respectively (Fig. 2).

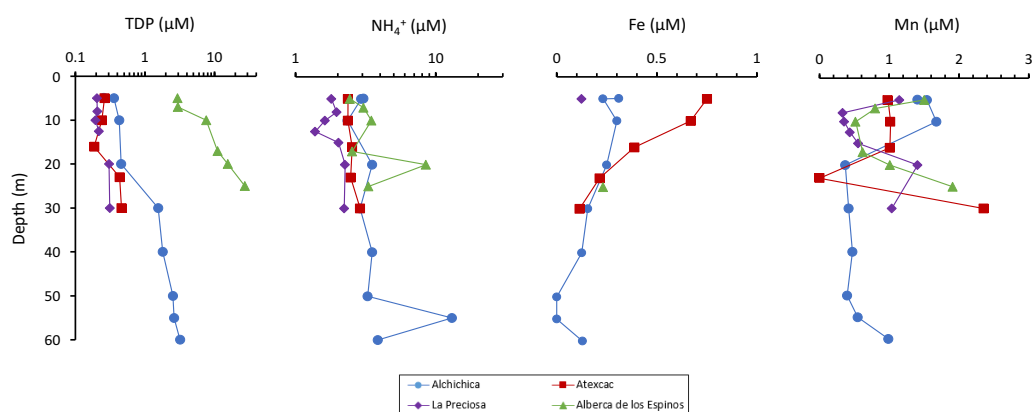
376 DIC represented about 91 % of all carbon present (DIC+DOC+POC) in the water column. Its concentration  
377 progressively increased from  $6.8 \text{ mM}$  at 5 m to  $7.2 \text{ mM}$  between 10 and 17 m. It further increased to  $8.7 \text{ mM}$  down  
378 to 26 m (Fig. 3, Table 2). The  $\delta^{13}\text{C}_{\text{DIC}}$  was about  $-2.4 \text{ ‰}$  between the surface and 7 m in depth, decreased to  $-4.1$   
379  $\text{‰}$  at 10 m, and increased back up to  $-2 \text{ ‰}$  at 25 m. POC represented about 0.5 % of the total carbon measured in  
380 the water column with a concentration of  $0.04 \text{ mM}$  at the surface decreasing to  $0.02 \text{ mM}$  at 10 m and increasing  
381 back to  $0.05 \text{ mM}$  in the hypolimnion. C:N ratio of POM progressively decreased from 8.5 at the surface to below  
382 6.5 in the hypolimnion.  $\delta^{13}\text{C}_{\text{POC}}$  had minimum values at 10 and 17 m ( $-28.3$  and  $-29 \text{ ‰}$ , respectively). Above and  
383 below,  $\delta^{13}\text{C}_{\text{POC}}$  was around  $-26.4 \text{ ‰}$ . DOC represented about 8 % of the total carbon, with a concentration around  
384  $0.4 \text{ mM}$  throughout the water column except at 7 and 17 m where DOC peaked to 1 and  $1.7 \text{ mM}$ , respectively (Fig.  
385 3). Its isotopic composition was mostly comprised between  $-27$  and  $-25 \text{ ‰}$  except at 7 m where it reached  $-15 \text{ ‰}$   
386 (Fig. 4). Total C concentration increased downward from about 7 to  $9 \text{ mM}$  (Fig. 3).  $\delta^{13}\text{C}_{\text{total}}$  decreased from  $-3.9$   
387 to  $-7.9 \text{ ‰}$  between 5 and 17 m and then increased up to  $-3.2 \text{ ‰}$  at 25 m (Fig. 4).

388 Total dissolved phosphorus increased from  $2.9$  to  $27.4 \mu\text{M}$  between 5 and 25 m (Fig. 5, Table S1). Dissolved  
389 sulfates as measured by chromatography were only detectable at 5 m with a low concentration of  $12 \mu\text{M}$ , while



390 total dissolved S measured by ICP-AES showed values in the hypolimnion higher than in the upper layers (~ 10.3  
391 vs 7.4  $\mu\text{M}$ , Table S1). Dissolved Cl slightly decreased from 4.25 to 4 mM between 5 and 10 m, before increasing  
392 back to 4.2 mM at 25 m. Dissolved Mn concentrations decreased from 1.5 to 0.5  $\mu\text{M}$  between 5 and 10 m, then  
393 increased to 2  $\mu\text{M}$  at 25 m. Aqueous Fe was only detectable at 25 m with a concentration of 0.23  $\mu\text{M}$  (Fig. 5, Table  
394 S1). In parallel, particulate S concentrations increased with depth, with a marked increase from 0.1 to 0.6  $\mu\text{M}$   
395 between 20 and 25m. This was spatially correlated with a 25-fold increase in particulate Fe (from 0.2 to 5.97  $\mu\text{M}$ ).  
396 Particulate Mn showed a peak between 17 and 20 m around 1  $\mu\text{M}$ , contrasting with values lower than 0.06  $\mu\text{M}$   
397 above 10 m and lower than 0.15 below 20 m (Fig. 2, Table S3).

398 In the first centimeters of the sediments, porewater DIC concentration and  $\delta^{13}\text{C}_{\text{DIC}}$  varied between ~ 11 and 12 mM  
399 and between +8 and +10 ‰, respectively. Sedimentary organic matter had a  $\delta^{13}\text{C}_{\text{SOC}}$  globally increasing from -  
400 29.4 to -25.5 ‰ and a C:N ratio varying between 11.6 and 14.3 (Figs. 3, 4; Table S2). Surficial sedimentary  
401 carbonates had a  $\delta^{13}\text{C}_{\text{CaCO}_3}$  around -1.5 ‰.



402 Figure 5. Concentrations of dissolved nutrients in micromoles.L<sup>-1</sup> in the water columns of the four lakes as a  
403 function of depth. TDP and TDS stands for ‘total dissolved P’ and ‘S’, respectively, and were measured by ICP-  
404 AES. Fe and Mn were measured by ICP-MS. Nitrogen species were measured by colorimetry.

405

406

## 407 5. DISCUSSION

408

### 409 5.1. General factors influencing the C cycle across the Mexican crater lakes

410

#### 411 5.1.1. The alkalinity gradient

412 Salinity and alkalinity (roughly equal to DIC) gradually increase from Lake La Alberca de los Espinos (~0.6 psu  
413 and 7 mM) to Alchichica (~7.9 psu and 35 mM), while lakes La Preciosa and Atexcac have intermediate values of  
414 1.15 and 7.44 psu and 13 and 26 mM, respectively (Table 1 and 2, Zeyen et al., 2021). The DIC gradient along  
415 which these four lakes distribute can be linked with different concentration stages of an initial dilute alkaline water  
416 (Zeyen et al., 2021), those different concentration stages being ultimately controlled by the different hydrological  
417 regimes of the lakes. First, the weathering of Cretaceous limestone in the SOB (with a  $\delta^{13}\text{C}$  around  $2 \pm 1$  ‰;  
418 Armstrong-Altrin et al., 2011; Núñez Useche et al., 2014) together with basaltic/andesitic bedrock (Armienta et



419 al., 2008; Carrasco-Núñez et al., 2007; Lelli et al., 2021) favors the inflow of more alkaline and DIC-concentrated  
420 groundwaters than in Lake La Alberca which lies on a purely basaltic basement (Rendon-Lopez, 2008; Siebe et  
421 al., 2014; Zeyen et al., 2021). Second, the SOB area presently experiences higher evaporation than precipitation  
422 rates (Alcocer, 2021), probably playing an important role in concentrating solutes and decreasing the water level  
423 in lakes Atexcac, Alchichica and La Preciosa (Anderson and Stedmon, 2007; Zeyen et al., 2021). Consistently,  
424 substantial “sub-fossil” microbialite deposits emerge above the current water level in lakes Alchichica and  
425 Atexcac, evidencing some significant lake level decrease (by up to 15 m in Lake Atexcac, *i.e.* ~40% of today’s  
426 lake maximum depth; and by about 3 m in Alchichica). Patches of emerged microbialites are also found in Lake  
427 La Preciosa. By contrast, emerged microbialites are almost not observed in Lake La Alberca de los Espinos  
428 (Fig. S1).

429 Additional local parameters, such as varying groundwater paths and fluxes (Furian et al., 2013; Mercedes-Martin  
430 et al., 2019; Milesi et al., 2020; Zeyen et al., 2021), most likely play a role in explaining part of the variations in  
431 DIC concentration between lakes. For example, Lake La Preciosa’s water composition significantly differs from  
432 that of Lake Alchichica and Atexcac, despite a similar geological context and climate (all located within 50 km<sup>2</sup>,  
433 Fig. 1). This could be explained by the fact that groundwaters in the SOB area become more saline as they flow  
434 towards the center of the basin and through the crater lakes (Silva Aguilera, 2019; Alcocer, 2021). Since  
435 groundwaters flow through La Preciosa first, they are more concentrated as they enter Alchichica than when they  
436 enter La Preciosa (Silva Aguilera, 2019; Alcocer, 2021; Lelli et al., 2021). Distinct regimes of volcanic CO<sub>2</sub>  
437 degassing into these crater lakes may also contribute to variations of the C mass balance between the four lakes.  
438 Last, different remineralization rates of organic carbon could also be a source of heterogeneity between the lakes  
439 DIC content. However, assuming that all POC and DOC ultimately remineralize into DIC, it would only represent  
440 a relatively small portion of the total carbon (16 % in Lake Atexcac, 9 % in Lake La Alberca de los Espinos and  
441 ~5 % for lakes Alchichica and La Preciosa). From an isotopic mass balance perspective, the  $\delta^{13}\text{C}_{\text{DIC}}$  of the three  
442 SOB lakes lie very far from  $\delta^{13}\text{C}_{\text{POC}}/\delta^{13}\text{C}_{\text{DOC}}$  signatures (Fig. 4), whereas Lake La Alberca exhibits more negative  
443  $\delta^{13}\text{C}_{\text{DIC}}$ , slightly closer to OC signatures (Fig. 4). This latter lake also stands out from the others because of the  
444 dense vegetation which surrounds it (Fig. S1). Therefore, La Alberca seems to be the only lake where OC  
445 respiration could be a significant source of inorganic C.

446 Mean  $\delta^{13}\text{C}_{\text{DIC}}$  values of the lakes broadly correlate with their alkalinity/salinity. This relationship is expected as  
447 evaporation generally increases the  $\delta^{13}\text{C}_{\text{DIC}}$  of residual water, notably because it increases lake pCO<sub>2</sub> and primary  
448 productivity which bolsters CO<sub>2</sub> degassing and organic C burial, both having low  $\delta^{13}\text{C}$  compared to DIC (e.g. Li  
449 and Ku, 1997; Talbot, 1990). By controlling the DIC speciation (H<sub>2</sub>CO<sub>3</sub>/CO<sub>2(aq)</sub>, HCO<sub>3</sub><sup>-</sup>, CO<sub>3</sub><sup>2-</sup>), pH also strongly  
450 influences  $\delta^{13}\text{C}_{\text{DIC}}$  because there is a fractionation of up to ~9 ‰ between the different DIC species (Emrich et al.,  
451 1970; Mook et al., 1974; Bade et al., 2004). Consistently, the  $\delta^{13}\text{C}_{\text{DIC}}$  of Mexican lakes are in the expected range  
452 for lakes with a pH around 9 (Bade et al., 2004), where DIC is dominated by HCO<sub>3</sub><sup>-</sup>. However, the pH values of  
453 the studied Mexican lakes are too close to each other to explain the significant difference observed between their  
454  $\delta^{13}\text{C}_{\text{DIC}}$  (Fig. 4;  $p=4.2\times 10^{-3}$  for Lakes Atexcac and La Preciosa which have the closest  $\delta^{13}\text{C}_{\text{DIC}}$ ). Last, lakes with  
455 lower DIC concentrations are expected to have a  $\delta^{13}\text{C}_{\text{DIC}}$  more easily influenced by exchanges with other carbon  
456 reservoirs, such as organic carbon (through photosynthesis/respiration) or other DIC sources (e.g., depleted  
457 volcanic CO<sub>2</sub> or groundwater DIC) – compared with buffered, high DIC lakes (Li and Ku, 1997; Fig. S3). This  
458 illustrates another (indirect) influence of the inter-lake chemical gradient on  $\delta^{13}\text{C}_{\text{DIC}}$ .



459 Therefore, the alkalinity gradient and to a first order, the size, isotopic composition and responsiveness of the DIC  
460 reservoir to biogeochemical processes are controlled by the local hydro-physico-chemical parameters of the lakes.

461

#### 462 5.1.2. Stratification of the lakes

463 Stratified water columns can sustain strong physico-chemical gradients, where a wide range of biogeochemical  
464 reactions impacting the C cycle can take place (e.g. Jézéquel et al., 2016). Here, temperature, conductivity and O<sub>2</sub>  
465 profiles show that the four lakes were clearly stratified at the time of sampling and had a similar general structure,  
466 although depths defining the successive epi-, meta- and hypolimnion layers differ between the lakes (Fig. 2). For  
467 example, we found a clear offset in Lake Alchichica and Lake La Alberca between the depth of O<sub>2</sub> depletion and  
468 the depth below which the ORP decreases. By contrast, ORP sharply dropped below the depth where O<sub>2(aq)</sub>  
469 disappeared in Atexcac and La Preciosa. Meanwhile, in all four lakes the ORP decreased below the depth where  
470 chlorophyll a peaks collapsed. This pigment being a tracer of oxygenic photosynthesis, it suggests that ORP was  
471 buffered at a high value by photosynthetically produced oxygen during C fixation and only decreased at a depth  
472 where aerobic respiration became higher than oxygenic photosynthesis. The offset between the ORP drop and O<sub>2</sub>  
473 depletion in Lake Alchichica and Alberca could result from more extended peaks of chlorophyll a that we can  
474 observe in these two lakes (Fig. 2). The exact factors causing this distribution of oxygenic primary producers  
475 remain to be determined. In the end nonetheless, this impacts the depth distribution of other microbial metabolisms  
476 that thrive at different redox levels as well as the depths at which authigenic particles precipitate following redox  
477 reactions, as exemplified by the depth profiles of turbidity and the particulate metal concentrations (Fig. 2).

478 The evolution of pH with depth is another example of the interplay between physico-chemical stratification of the  
479 lakes and their respective C cycle. pH showed a stratified profile in La Preciosa and La Alberca, whereas it  
480 remained constant in Alchichica and Atexcac. The pH decline at the oxycline of Lake La Preciosa was associated  
481 with the decrease of DOC, POC and chlorophyll a concentrations and  $\delta^{13}\text{C}_{\text{DIC}}$  values, reflecting the high impact of  
482 oxygen respiration (i.e. carbon remineralization) at this depth (Figs. 2-4). In Lake La Alberca, the surface waters  
483 are markedly more alkaline than the bottom waters, with a two-step decrease of pH occurring at around 8 m and  
484 17 m (total drop of 1.5 pH unit). Based on the same observations as in La Preciosa, this likely results from high  
485 OM respiration, although input of volcanic acidic gases (e.g. dissolved CO<sub>2</sub>) might also contribute to the pH  
486 decrease in the bottom waters, as reflected by negative  $\delta^{13}\text{C}_{\text{DIC}}$  signatures and the increase of [DIC] and  
487 conductivity in the hypolimnion (Figs. 2-4). By contrast, while the same pieces of evidence for oxygen respiration  
488 ([POC], chlorophyll, etc.) can be detected in the two other lakes, this did not similarly impact their pH profile  
489 (Fig. 2). This suggests that the acidity generated by these reactions is buffered by the much higher alkalinity  
490 measured in these two lakes. Thus, external constraints on the alkalinity buffering capacity of these lakes (e.g.,  
491 lake hydrology, fluid sources, Sect. 5.1.1) influence their vertical pH profile, which is particularly important  
492 considering the critical interplay between pH and biogeochemical reactions affecting the C cycle (e.g. Soetaert et  
493 al., 2007).

494 In summary, although the four lakes present the same general structure and environmental conditions, external  
495 factors (such as hydrology, fluid sources or stratification characteristics) result in contrasting compositions of their



496 water chemistries, which in turn, has a critical impact on the physico-chemical depth profiles of each lake and their  
497 biogeochemical carbon cycle functioning.

498

## 499 **5.2. From water column primary production to sedimentary organic matter: insights from POC and** 500 **DIC signatures**

501

502 In this section, we discuss the different biological processes that can be evidenced based on the depth variations  
503 of DIC and POM chemical and isotopic compositions.

### 504 **5.2.1. Primary productivity by oxygenic photosynthesis in the upper water column**

505 All four crater lakes are endorheic basins, i.e. there is no surface water inflow or outflow. Therefore, the organic  
506 carbon sources are predominantly autochthonous, mainly resulting from planktonic autotrophic C fixation. This is  
507 supported by C:N ratios of POM that were comprised between 6 and 12 in the four lakes, i.e., close to the Redfield  
508 but far from land plant ratios. Abundant vegetation covers the crater walls of Lake Alberca and to a lesser extent  
509 Lake Atexcac; some plant debris were observed and sampled in the sediment cores of these two lakes. They had  
510 high C:N ratios, typical of plant tissues (between 24 and 68) and significantly higher than those of the bulk organic  
511 matter of surficial sediments (between 8 and 13) and the water column (between 6 and 12) (Fig. 3). Therefore,  
512 local allochthonous organic carbon in these two lakes – albeit present – does not significantly contribute to their  
513 bulk organic signal.

514 The importance of planktonic autotrophic C fixation as a major source of organic C in the four lakes is further  
515 supported by the assessment of the isotopic discrimination between DIC and organic biomass, expressed as  
516  $\Delta^{13}\text{C}_{\text{POC-DIC}}$  and  $\epsilon_{\text{POC-CO}_2}$  (Table 3).  $\Delta^{13}\text{C}_{\text{POC-DIC}}$  vary between -29 and -23 ‰ (corresponding to  $\epsilon_{\text{POC-CO}_2}$  between -  
517 20 and -14 ‰; Table 4) throughout the four water columns, which is in the typical range of planktonic oxygenic  
518 phototrophs (Pardue et al., 1976; Sirevag et al., 1977; Thomas et al., 2019). Yet, these values exhibit variability –  
519 both within a single water column (up to 4.5 ‰) and between the different lakes (up to 6 ‰, Figs 4 and 6) – which  
520 could trace several abiotic and biotic factors.

521 Notably, higher DIC availability in Alchichica and Atexcac probably makes the carboxylation step more limiting  
522 during photosynthesis (e.g. O’Leary, 1988; Descolas-Gros and Fontugne, 1990; Fry, 1996) and increase  $|\Delta^{13}\text{C}_{\text{POC-}}$   
523  $\text{DIC}|$  in these lakes compared to La Preciosa and Alberca (Fig. 6a; between 24 and 27 ‰ for these two lakes *versus*  
524 28 to 29.5 ‰ for Alchichica and Atexcac, at the peak of Chl. a). Indeed, lower  $\text{CO}_{2(\text{aq})}$  availability and/or higher  
525 reaction rates result in transport-limited rather than carboxylation-limited uptake and thus, smaller C isotope  
526 fractionation between POC and DIC (Pardue et al., 1976; Zohary et al., 1994; Fry, 1996; Close and Henderson,  
527 2020). This is because the isotopic fractionation associated with diffusion is much smaller than with carboxylation  
528 and because a higher proportion of the DIC entering the cells is converted into organic biomass (e.g. Fogel and  
529 Cifuentes, 1993). Consistently, we notice a correlation among the lakes between  $a(\text{CO}_{2(\text{aq})}$ ) (or [DIC]) and  $|\epsilon_{\text{POC-}}$   
530  $\text{CO}_2|$  at depths where oxygenic photosynthetic peaks (Fig. S4). Furthermore, Lakes La Preciosa and Alberca are  
531 considered more eutrophic than the two other lakes (Lugo et al., 1993; Vilaclara et al., 1993; Callieri et al., 2013)  
532 consistently with higher chlorophyll a content and photosynthetic rates and thus smaller  $|\Delta^{13}\text{C}_{\text{POC-DIC}}|$ . Additionally,



533 higher water temperatures in Alberca de los Espinos (by ~ 3 °C) could partly contribute to smaller  $|\Delta^{13}\text{C}_{\text{POC-DIC}}|$  in  
 534 this lake (Sackett et al., 1965; Pardue et al., 1976; Descolas-Gros and Fontungne, 1990).

535 Unlike  $\delta^{13}\text{C}_{\text{DIC}}$ , organic carbon isotopic signatures do not evolve linearly with the alkalinity/salinity gradient,  
 536 suggesting other lake- and microbial-specific controls on these signatures. These include: diffusive or active uptake  
 537 mechanisms, specific carbon fixation pathways, the fraction of intracellular inorganic carbon released out of the  
 538 cells, cell size and geometry (Werne and Hollander, 2004 and references therein) and remineralization efficiency.  
 539 Moreover, an increasing number of isotopic data has evidenced a significant variability of the isotopic fractionation  
 540 achieved by different purified RuBisCO enzymes ( $\epsilon_{\text{RuBisCO}}$ , Iñiguez et al., 2020), and even by a single RuBisCO  
 541 form (Thomas et al., 2019). Thus, caution should be paid to the interpretation of the origin of small isotopic  
 542 variations of the biomass in distinct environmental contexts because RuBisCO alone can be an important source  
 543 of this variability (Thomas et al., 2019).

544

545 Table 3

546 Index for mathematical notations used in the text including C isotopic composition of a reservoir X ( $\delta^{13}\text{C}_X$ ),  
 547 isotopic discrimination between the two carbon reservoirs X and Y ( $\Delta^{13}\text{C}_{X-Y}$ ). In the main text, we report organic  
 548 C isotopic discrimination *versus* both bulk DIC ( $\Delta^{13}\text{C}_{\text{POC-DIC}}$ ) – in a way to facilitate studies intercomparison and  
 549 because it is the commonly reported raw measured data (Fry, 1996) – and calculated  $\text{CO}_{2(\text{aq})}$  ( $\epsilon_{\text{POC-CO}_2}$ ) in order to  
 550 discuss the intrinsic isotopic fractionations associated with the lakes metabolic diversity. All C isotope values and  
 551 fractionations are reported relative to the international standard VPDB (Vienna Pee Dee Belemnite).

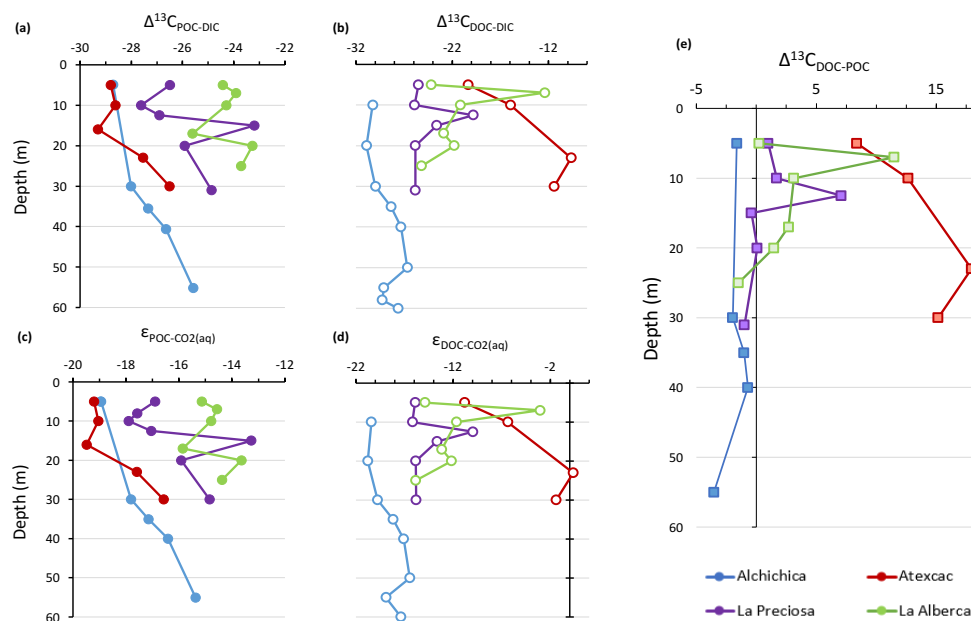
Symbols	Mathematical Expression	Signification
$\delta^{13}\text{C}_X$	$\left( \frac{\left( \frac{^{13}\text{C}}{^{12}\text{C}} \right)_X}{\left( \frac{^{13}\text{C}}{^{12}\text{C}} \right)_{\text{VPDB}}} - 1 \right) * 1000$	Relative difference in $^{13}\text{C}:^{12}\text{C}$ isotopic ratio between a sample of a given C reservoir and the international standard "Vienna Pee Dee Bee", expressed in permil (‰). $\delta^{13}\text{C}_{\text{total}}$ represents the weighted average of $\delta^{13}\text{C}$ for all DIC, DOC and POC.
$\Delta^{13}\text{C}_{X-Y}$	$= \delta^{13}\text{C}_X - \delta^{13}\text{C}_Y \approx 1000/\alpha_{X-Y}$	Apparent isotopic fractionation between two reservoirs 'X' and 'Y'. Difference between their measured C isotope compositions approximating the fractionation $\alpha$ in ‰.
$\epsilon_{X-\text{CO}_2}$	$= (\alpha_{X-\text{CO}_2} - 1)1000 \approx \delta^{13}\text{C}_X - \delta^{13}\text{C}_{\text{CO}_2}$	Calculated isotopic fractionation between a reservoir 'X' and $\text{CO}_{2(\text{aq})}$ . $\alpha_{X-\text{CO}_2}$ is calculated as $(\delta^{13}\text{C}_X+1000)/(\delta^{13}\text{C}_{\text{CO}_2}+1000)$ where $\delta^{13}\text{C}_X$ is measured and $\delta^{13}\text{C}_{\text{CO}_2}$ is computed based on DIC isotopic composition and speciation (see supplementary information).
Indexes	DIC DOC POC SOC	Dissolved Inorganic- , Dissolved Organic- , Particulate Organic- , Sedimentary Organic-Carbon

552

553

### 554 5.2.2. Aerobic respiration at the oxycline

555 At the oxycline of stratified water bodies, aerobic respiration of OM by heterotrophic organisms favors the  
 556 transition from oxygenated upper layers to anoxic bottom waters. In the water column of the four lakes,  $\Delta^{13}\text{C}_{\text{POC-}}$   
 557 DIC (and  $\epsilon_{\text{POC-CO}_2}$ ) show increasing values in the hypolimnion, and especially below the chlorophyll a peaks (Fig. 2;  
 558 6). This trend also correlates with increasing  $\delta^{13}\text{C}_{\text{POC}}$ , decreasing (C:N)<sub>POM</sub> ratios as well as decreasing POC



559

Figure 6. Isotopic fractionations between POC and DIC, DOC and DIC, DOC and POC in the water columns of the four lakes, expressed as  $\Delta^{13}\text{C}_{x-y}$ . Refer to Table 3 for more detail about the  $\Delta$  notation.

560 concentrations (except in La Alberca) (Figs 3 and 4). Decreasing POC concentrations near the oxycline and  
 561 redoxcline are consistent with the fact that part of the upper primary production is degraded deeper in the water  
 562 columns and/or that there is less primary production in the anoxic bottom waters. Increase of  $\delta^{13}\text{C}_{\text{POC}}$  in the  
 563 hypolimnion of the lakes is consistent with heterotrophic activity and points out that POC at these depths could  
 564 mainly record secondary production rather than sinking degraded primary production. Indeed, heterotrophic  
 565 bacteria preferentially grow on available  $^{13}\text{C}$ -enriched amino acids and sugars, thus becoming more enriched than  
 566 their C source (Williams and Gordon, 1970; Hayes et al., 1989; Zohary et al., 1994; Briones et al., 1998; Lehmann  
 567 et al., 2002; Jiao et al., 2010; Close and Henderson, 2020). Decreasing C:N ratios in POM also reinforce that  
 568 conclusion since secondary heterotrophic bacteria biomass generally have C:N between 4 and 5 (Lehmann et al.,  
 569 2002). By contrast, residual OM from primary producers degraded by heterotrophs would carry higher C:N  
 570 signatures (van Mooy et al., 2002; Buchan et al., 2014) that are not recorded by POM in the lower water columns  
 571 of the lakes (Fig. 3). In Lake La Preciosa, the water column shifts from a highly oxygenated state to anoxia in a  
 572 ~5 m interval against more than 10 m for Alchichica and Atexcac. This correlates with a sharp  $\delta^{13}\text{C}_{\text{POC}}$  increase (+  
 573 3.4‰) at 15 m, highlighting how efficient and  $\text{O}_2$ -dependent the remineralization process is in this lake.

574 The  $\delta^{13}\text{C}_{\text{DIC}}$  signatures in lakes Alchichica and La Preciosa are consistent with the mineralization of OM as they  
 575 exhibit lower values below the oxycline than in surficial waters (Figs 2; 4). Similarly to what is observed in several  
 576 other water bodies and notably stratified water columns such as the Black Sea (e.g. Fry et al., 1991), surface  
 577 photosynthesis increases  $\delta^{13}\text{C}_{\text{DIC}}$  by fixing light DIC, while respiration transfers light OC back to the DIC pool at  
 578 depth. Such a decrease of the  $\delta^{13}\text{C}_{\text{DIC}}$  can also be seen in the oxycline of Lake La Alberca between 7 and 10 m.



579 Table 4  
 580 Isotopic fractionations between dissolved inorganic and organic carbon (DIC, DOC) and particulate organic carbon  
 581 (POC), where  $\Delta^{13}C_{x-y} = \delta^{13}C_x - \delta^{13}C_y$  is the apparent fractionation and  $\epsilon$  is computed as the actual metabolic isotopic  
 582 discrimination between CO<sub>2</sub> and POC/DOC (see Table 3).  $\delta^{13}C_{DOC}$  was not measured at 5 m depth and its value at  
 583 10 m was used in this calculation of  $\Delta^{13}C_{DOC-POC}$ .

Lake	Sample	$\Delta^{13}C_{POC-DIC}$	$\Delta^{13}C_{DOC-DIC}$	$\Delta^{13}C_{DOC-POC}$	$\epsilon_{POC-DIC}$	$\epsilon_{DOC-DIC}$
		‰			‰	
Alchichica	AL 5m	-28.7		-1.6*	-19.1	
	AL 10m		-30.3			-20.4
	AL 20m		-30.9			-20.6
	AL 30m	-28.0	-30.0	-2.0		-20.9
	AL 35m	-27.3	-28.4	-1.0	-17.9	-19.9
	AL 40m	-26.6	-27.3	-0.7	-17.3	-18.3
	AL 50m		-26.7		-16.5	-17.2
	AL 55m	-25.6	-29.1	-3.5		-16.6
	AL 58m		-29.3		-15.5	-19.0
	AL 60m		-27.6			-17.5
Atexcac	ATX 5m	-28.8	-20.4	8.4	-19.3	-10.9
	ATX 10m	-28.6	-16.0	12.6	-19.1	-6.5
	ATX 16m	-29.3			-19.5	
	ATX 23m	-27.5	-9.7	17.9	-17.6	0.3
	ATX 30m	-26.5	-11.4	15.2	-16.6	-1.5
La Preciosa	LP 5m	-26.5	-25.5	1.0	-16.9	-15.9
	LP 10m	-27.6	-25.9	1.7	-17.9	-16.2
	LP 12.5m	-26.9	-19.8	7.1	-17.1	-10.0
	LP 15m	-23.2	-23.6	-0.4	-13.3	-13.7
	LP 20m	-25.9	-25.8	0.1	-15.9	-15.9
	LP 31m	-24.9	-25.8	-1.0	-14.9	-15.8
La Alberca de Los Espinos	Albbsp 5m	-24.4	-24.2	0.2	-15.2	-15.0
	Albbsp 7m	-23.9	-12.4	11.5	-14.6	-3.1
	Albbsp 10m	-24.3	-21.2	3.1	-14.8	-11.7
	Albbsp 17m	-25.6	-22.9	2.7	-15.9	-13.2
	Albbsp 20m	-23.3	-21.8	1.5	-13.6	-12.2
	Albbsp 25m	-23.7	-25.2	-1.5	-14.4	-15.9

584

585

### 586 5.2.3. Primary production in the hypolimnion

587 Anoxygenic autotrophs commonly thrive in anoxic bottom waters of stratified water bodies (e.g. (Pimenov et al.,  
 588 2008; Zyakun et al., 2009; Posth et al., 2017; Fulton et al., 2018; Havig et al., 2018). They have been identified at  
 589 different depths in the four Mexican lakes (Macek et al., 2020; Iniesto et al., in press). Based on our results obtained  
 590 on samples collected during the stratification period, anoxygenic autotrophs appear to have an impact on the C  
 591 cycle of lakes Atexcac and La Alberca only. Lake Atexcac records a concomitant decrease of [DIC] and increase  
 592 of  $\delta^{13}C_{DIC}$  in the anoxic hypolimnion at 23 m, below the peak of chlorophyll a, suggesting autotrophic C fixation  
 593 by chemoautotrophy or anoxygenic photosynthesis. The calculated  $\epsilon_{POC-CO_2}$  at 23 m (-17.5 ‰) is consistent with  
 594 C isotopes fractionation by purple- and green sulphur-anoxygenic bacteria (PSB and GSB), while  $\epsilon_{POC-CO_2}$  in La  
 595 Alberca's hypolimnion (~ -15 ‰) is closer to GSB canonical signatures (Posth et al., 2017 and references therein)  
 596 (Fig. 6c). In La Alberca, anoxygenic primary productivity is moreover suggested by increasing POC



597 concentrations. Besides, we also observe a Chl. *a* peak in the anoxic hypolimnion of this lake (Fig. 2), which likely  
598 represents a bias of the probe towards some bacteriochlorophylls typical of GSB (see supplementary information).  
599 We notice that in Lake Atexcac, C fixation at 23 m by anoxygenic autotrophs causes a shift in the DIC reservoir,  
600 while oxygenic photosynthesis at 16 m does not, suggesting that anaerobic autotrophs are the main autotrophic  
601 metabolisms in this lake (in terms of DIC uptake). In La Alberca, the increase of [POC] to maximum values at  
602 depth also supports the predominance of anoxygenic versus oxygenic autotrophy (Fig. 3). This is similar with other  
603 stratified water bodies which exhibit primary production clearly dominated by anoxygenic metabolisms (Fulton et  
604 al., 2018).

605 Furthermore, at 23 m in Lake Atexcac and 17 m in Lake La Alberca, we find a striking turbidity peak precisely  
606 where the redox potential and concentrations of dissolved Mn drop (Fig. 2). In Lake Atexcac concentrations of  
607 dissolved metal such as Cu, Pb or Co also drop at 23 m (Fig. S5). In La Alberca, a peak of particulate Mn  
608 concentrations is also detected at 15 m (Fig. 2; data not available for Atexcac). This is most likely explained by  
609 the precipitation of Mn as oxide particles where reduced bottom waters meet oxidative conditions prevailing in  
610 the upper waters. Such Mn-oxides, even at low  $\mu\text{M}$  concentrations, can catalyze abiotic oxidation of sulfide to  
611 sulfur compounds (van Vliet et al., 2021), which in turn can be used and further oxidized to sulfate by phototrophic  
612 or chemoautotrophic sulfur-oxidizing bacteria. This is also consistent with the small increase of  $[\text{SO}_4^{2-}]$  observed  
613 at 23 m in Atexcac (Table S1). Besides Mn-oxides can be used as electron acceptors during chemoautotrophy  
614 (Havig et al., 2015; Knossow et al., 2015; Henkel et al., 2019; van Vliet et al., 2021).

615

#### 616 **5.2.4. Influence of methanogenesis and volcanic- $\text{CO}_2$ degassing from the sediments of Lake La** 617 **Alberca de los Espinos**

618 Lake La Alberca shows the least saline/alkaline water column and most peculiar geochemical depth profiles among  
619 the four lakes. Notably, its [DIC] and  $\delta^{13}\text{C}_{\text{DIC}}$  (the lowest of the studied lakes) increase from the lower metalimnion  
620 to the hypolimnion and further into the pore waters of the first cm of sediments with  $\delta^{13}\text{C}_{\text{DIC}}$  reaching up to  $\sim 11$  ‰  
621 (Figs. 3, 4). Consistently, the calculated  $\text{CO}_2$  partial pressure ( $P_{\text{CO}_2}$ ) increases downward from slightly less than 1x  
622 that of atmospheric  $P_{\text{CO}_2}$  near the lake surface up to almost 40x at the bottom of the lake (Table S4). The total  
623 carbon concentration depicts a clear increase from surface waters to the bottom of the lake (Fig. 3).

624 While the increase of [POC] at depth may contribute to the observed  $\delta^{13}\text{C}_{\text{DIC}}$  increase by mass balance, it should  
625 also lower the [DIC] instead of increasing it. Similarly, the sinking of OC particles at depth followed by their  
626 remineralization into DIC cannot explain those observations since this would lower the  $\delta^{13}\text{C}_{\text{DIC}}$  in the hypolimnion  
627 (Fig. 4). Overall, these observations require that a significant source of inorganic  $^{13}\text{C}$ -rich carbon fuels the bottom  
628 waters of Alberca de los Espinos. The source of heavy carbon most likely results from methanogenesis, which  
629 consumes organic carbon in the sediments and produces  $^{13}\text{C}$ -depleted methane and  $^{13}\text{C}$ -rich carbon dioxide  
630 diffusing upward in the water column (acetoclastic methanogenesis, dominant in lacustrine contexts, Whiticar et  
631 al., 1986). Methanogenesis, as an “alternative” OM remineralization pathway could be favored in Lake La Alberca,  
632 because this lake is relatively rich in OM (notably with high [DOC]), and depleted in  $\text{SO}_4$  compared with the three  
633 other Mexican lakes (Wittkop et al., 2014; Birgel et al., 2015; Cadeau et al., 2020). Based on the isotopic  
634 compositions of sedimentary organic carbon and porewater DIC in Lake La Alberca, we can tentatively calculate



635 the methane isotopic signature (see supplementary information). The calculated  $\delta^{13}\text{C}_{\text{CH}_4}$  in the first 10 cm of  
636 sediments is between -59 and -56.8 ‰, which is consistent with biogenic methane (Whiticar et al., 1986).

637 Upward diffusing methane may be either (i) partly lost from the lake's surface (i.e. escaping the system) by  
638 degassing or (ii) totally kept in the water column by complete oxidation (either abiotically by oxygenated surface  
639 waters or biologically by methanotrophic organisms). The oxidation of  $\text{CH}_4$  in the water column should lead to the  
640 formation of  $^{13}\text{C}$ -depleted carbon dioxide that would mix back with the lake DIC (and notably with heavy  
641 methanogenic  $\text{CO}_2$  produced at depth) as well as  $^{13}\text{C}$ -depleted biomass (as POC or SOC) if it occurs by  
642 methanotrophy. Thus, the net effect of combined methanogenesis and methane oxidation is expected to (i) generate  
643 a  $\delta^{13}\text{C}_{\text{DIC}}$  gradient from high to low values between the sediment porewaters and the chemocline as proposed  
644 elsewhere (Assayag et al., 2008; Wittkop et al., 2014) and (ii) progressively lower sedimentary  $\delta^{13}\text{C}_{\text{SOC}}$  in case of  
645 methanotrophy. Abiotic oxidation of methane by dioxygen is consistent with the observations that  $\delta^{13}\text{C}_{\text{DIC}}$   
646 decreases from porewaters ( $\sim +10$  ‰) to the chemocline ( $-4$  ‰), reaching minimum values where dissolved- $\text{O}_2$   
647 starts to appear (Fig. 2). On the other hand, microbial anaerobic methane oxidation (AMO) could occur at 17 m  
648 depth through Mn-oxides reduction (Cai et al., 2021; Cheng et al., 2021) and possibly bacterial sulfate-reduction  
649 closer to the water-sediment interface as inferred for the surficial sediments of meromictic Lake Cadagno (Posth  
650 et al., 2017). Indeed, we observe a net increase of particulate Fe and S concentrations at a depth of 25 m and a  
651 peak of solid sulfide minerals in the surficial sediments (Fig. S6). However,  $\delta^{13}\text{C}_{\text{SOC}}$  and  $\delta^{13}\text{C}_{\text{POC}}$  are far from  
652 calculated  $\delta^{13}\text{C}_{\text{CH}_4}$ , suggesting that AMO is not a major process in the bottom lake waters and surface sediments  
653 (Lehmann et al., 2004) and thus that methanotrophy is not the main  $\text{CH}_4$  oxidation pathway in Lake La Alberca.

654 Alternatively, if some portion of the methane escaped oxidation and degassed out of the lake,  $\delta^{13}\text{C}_{\text{DIC}}$  would likely  
655 be driven to extreme positive values with time, as observed elsewhere (Gu et al., 2004; Hassan, 2014; Birgel et al.,  
656 2015; Cadeau et al., 2020). This is not consistent with the observation that the average  $\delta^{13}\text{C}_{\text{DIC}}$  in Lake La Alberca  
657 is about -3 ‰ (Fig. 4), unless an additional counterbalancing source of DIC to this lake exist. In fact, we notice  
658 that  $\delta^{13}\text{C}_{\text{total}}$  averages -4.8‰ in Lake La Alberca, which is very similar to mantle- $\text{CO}_2$  signatures (Javoy et al.,  
659 1986; Mason et al., 2017). A contribution from mantle  $\text{CO}_2$  degassing in this lake may sustain a high  $\text{P}_{\text{CO}_2}$  and  
660 [DIC] at depth and maintain the lakes average  $\delta^{13}\text{C}_{\text{total}}$  close to a mantle isotopic signature and notably away from  
661 extreme positive values (if  $\text{CH}_4$ -escape dominated). Moreover, Lake La Alberca is located on top of a likely active  
662 normal fault (Siebe et al., 2012), which is favorable to the ascent of volcanic gases. It is also possible that volcanic  
663  $\text{CO}_2$  degassing is coupled to methanogenesis by  $\text{CO}_2$  reduction in addition to the acetoclastic one described above.  
664 We observe a strong pH decline at depth in this lake (mostly below 17 m, Fig. 2) which could be fostered by both  
665 the acidic volcanic gases (Pecoraino et al., 2015) and methanogenesis, although other redox and microbial  
666 reactions could impact the pH as well (Soetaert et al., 2007).

667 Overall, volcanic  $\text{CO}_2$  could be an important source in the C mass balance of Lake La Alberca. We note however,  
668 that volcanic  $\text{CO}_2$  alone cannot explain the very positive  $\delta^{13}\text{C}_{\text{DIC}}$  in the sediment porewaters. Only a future  
669 quantification of the fluxes of sedimentary methane production, volcanic  $\text{CO}_2$  and possible  $\text{CH}_4$  efflux out of the  
670 lake will help to better constraint the peculiar C cycle of Lake La Alberca.

671

672 **5.2.5. Which OM from the water column transfers to the surficial sediments?**



673 Although the nature and geochemical signatures of the OM that deposits in the bottom sediments may vary  
674 throughout the year, it is interesting to infer from what part(s) of the water column surficial sedimentary OM comes  
675 from during the stratified seasons.

676 In the three lakes from the SOB,  $\delta^{13}\text{C}$  and C:N signatures of the surficial sediments OM lie in between POM  
677 signatures from the upper water columns and from the hypolimnion (Figs. 3, 4). Nonetheless, in Alchichica, top  
678  $\delta^{13}\text{C}_{\text{SOC}}$  and  $(\text{C:N})_{\text{SOM}}$  signatures ( $-25.7\text{‰}$  and 10.5, respectively) lie much closer to values recorded in the upper  
679 water column ( $\sim -26.5\text{‰}$  and 10.5, respectively) implying that the upper oxygenic photosynthesis production is  
680 primarily recorded. In Lake Atexcac on the contrary,  $\delta^{13}\text{C}_{\text{SOC}}$  and  $(\text{C:N})_{\text{SOM}}$  signatures ( $\sim -27\text{‰}$  and 8,  
681 respectively) lie closer to values recorded in the hypolimnion ( $\sim -26.5\text{‰}$  and 6.5, respectively) suggesting that  
682 SOM records mostly the anaerobic primary production. Finally, in Lake La Alberca, surficial  $\delta^{13}\text{C}_{\text{SOC}}$  are markedly  
683 more negative (by  $\sim 2$  to  $3\text{‰}$ ) than the deepest and shallowest water column values (Fig. 4) but they are close to  
684 what is recorded at the redoxcline depth of 17 m. However, the  $(\text{C:N})_{\text{SOM}}$  values are much higher than what is  
685 measured in the water column, which is consistent with remineralization of OM by sulfate-reduction and  
686 methanogenesis in sediments of this lake (see also Sect. 1). Therefore, OM biogeochemical signatures in La  
687 Alberca's surficial sediments could mainly reflect the effect of early diagenesis occurring at the water-sediment  
688 interface. Importantly though, methanogenesis/methanotrophy are recorded in the surficial sediments porewaters  
689 (notably seen through extremely positive  $\delta^{13}\text{C}_{\text{DIC}}$ ) but not in the solid sediments that show neither very negative  
690  $\delta^{13}\text{C}_{\text{SOC}}$  nor positive  $\delta^{13}\text{C}_{\text{carbonates}}$  in the first 10 cm.

691 Overall, this suggests that OM depositing at the bottom of these stratified lakes do not always record geochemical  
692 signatures from the same sections of the water columns. Notably, they do not necessarily record the signatures of  
693 primary production by oxygenic photosynthesis from the upper column. For example, in Lake Atexcac,  
694 sedimentary OM records instead primary production by anoxygenic photosynthesis, even though POC  
695 concentration was maximum in the upper water column. In Lake La Alberca, OM is rapidly altered by diagenesis  
696 processes, but the signal of methanogenesis is not preserved in the sedimentary OM or carbonates, but only  
697 recorded by the sediment porewaters.

698

### 699 **5.3. A particularly large and central DOC reservoir**

700

701 In all four Mexican lakes studied here, the DOC reservoir occupies a predominant role, while showing quite diverse  
702 dynamics and characteristics between the lakes. Indeed, the four lakes have a high DOC content but very different  
703  $[\text{DOC}] / \delta^{13}\text{C}_{\text{DOC}}$  profiles and signatures despite quite similar ones for the DIC and POC reservoirs (Fig. 3; 4).  
704 Evaporation may be one process increasing DOC concentrations (Anderson and Stedmon, 2007; Zeyen et al.,  
705 2021). However, it is likely marginal here because on the contrary to what was observed for DIC, there is no  
706 correlation between the average  $[\text{DOC}]$  in the Mexican lakes and their salinity. Moreover, evaporation would not  
707 explain the significant intra-lake DOC depth variability.



708 In this section, we explore the different patterns of DOC production and fate, which depend on slight environmental  
709 and biological variations between the Mexican lakes. Moreover, we further describe the role of the DOC reservoir  
710 on other processes of the lakes C cycle and its potential implications in past oceans C cycle perturbations.

711

### 712 **5.3.1. Sources and fate of DOC**

713 Dissolved organic carbon is an operationally defined fraction of aqueous organic carbon (here separated from  
714 particulate organic carbon by filtration at 0.22  $\mu\text{m}$ ) within a continuum of organic molecules spanning a large  
715 range of sizes, compositions, degrees of reactivity and bioavailability (Kaplan et al., 2008; Hansell, 2013; Beaupré,  
716 2015; Carlson and Hansell, 2015; Brailsford, 2019). The endorheic nature of the studied lakes allows to specifically  
717 focus on the effects of autochthonous primary production, and notably its effects on the DOC reservoir.  
718 Autochthonous DOC can form through multiple processes broadly including: higher-rank OM degradation  
719 processes such as sloppy feeding by predators, UV photolysis or bacterial and viral cell lysis (Lampert, 1978;  
720 Hessen, 1992; Bade et al., 2007; Thornton, 2014; Brailsford, 2019) as well as passive (leakage) or active  
721 (exudation) release by healthy cells (e.g. Baines and Pace, 1991; Hessen and Anderson, 2008; Thornton, 2014;  
722 Ivanovsky et al., 2020). In general, this C release (either “active” or “passive”) tends to be enhanced in nutrient-  
723 limited conditions because some recently fixed C is in excess compared with other essential nutrients such as N or  
724 P (Hessen and Anderson, 2008; Morana et al., 2014; Ivanovsky et al., 2020). Moreover, oligotrophic conditions  
725 tend to limit heterotrophic bacterial activity and thus preserve the DOC stocks (Thornton, 2014; Dittmar, 2015).  
726 In the studied lakes, this may partly explain the trend of increasing DOC concentrations from the more eutrophic  
727 Lake Alberca and La Preciosa’s waters (0.7 mM on average) to the more oligotrophic Alchichica (1.8 mM) and  
728 Atexcac’s (6.5 mM).

729

#### 730 *DOC release by autotrophs*

731 In the four Mexican lakes, [DOC] depth profiles exhibit one or several peaks standing out from low background  
732 values and occurring both in oxic and anoxic waters (Fig. 3). In La Alberca and La Preciosa they correlate with  
733 chlorophyll a peaks. In the two other lakes, they do not match chlorophyll increase. However, in Atexcac, a  
734 remarkable DOC peak (over 10-fold increase, Fig. 3) occurs at the same depth as anoxygenic photosynthesis (Sect.  
735 5.2.3). These co-occurrences support that a large portion of DOC in these three lakes (at least at these depths) arise  
736 from the release of photosynthetic C fixed in excess. Phytoplankton release of DOM is generally thought to be  
737 carried out by (i) an active “overflow mechanism” (DOM exudation) or (ii) a passive diffusion throughout the cell  
738 membranes. In the first case, DOM is actively released out of the cells as a result of C fixation rates higher than  
739 growth and molecular synthesis rates (e.g. Baines and Pace, 1991). Hence, DOM exudation depends on  
740 environmental factors such as irradiance and nutrient availability (e.g. Morana et al., 2014). Besides, it may serve  
741 “fitness-promoting purposes” such as storage, defense or mutualistic goals (Hessen and Anderson, 2008). In the  
742 second case (passive diffusion), DOC release depends on cells permeability and the outward DOC gradient, and  
743 is more directly connected to the amount of phytoplankton biomass (e.g. Marañón et al., 2004). Thus, any new  
744 photosynthate production insures a steady DOM release rate, regardless of the environmental conditions (Marañón  
745 et al., 2004; Morana et al., 2014). In the studied lakes, the fact that lakes La Preciosa and Alberca have lower DOC



746 but overall higher chlorophyll a concentrations than Atexcac and Alchichica suggests that DOC production does  
747 not directly relate with phytoplankton biomass and is not passively released. Alternatively, an active DOC release  
748 is bolstered by DOC isotopic signatures (see below). Furthermore, the studied Mexican lakes precisely correspond  
749 to environmental contexts (high irradiance and oligotrophic freshwater bodies) where DOM exudation has been  
750 observed and is predicted (e.g. Baines and Pace, 1991; Morana et al., 2014; Thornton, 2014).

751 At depths where oxygenic photosynthesis occurs, the DOC over total OC ratio averages approximately 85, 99, 94  
752 and 95 % for lakes Alchichica, Atexcac, La Preciosa and La Alberca, respectively. Release of DOC by primary  
753 producers can be characterized by the percentage of extracellular release (PER), which corresponds to the fraction  
754 of DOM over total (dissolved and particulate) OM primary production (e.g. Thornton et al., 2014). PER is highly  
755 variable and averages about 13% of C biomass over a wide range of environments (e.g. Baines and Pace, 1991;  
756 Thornton, 2014). But values as high as 99% have been reported (see Bertilsson and Jones, 2003). Thus, although  
757 some of the DOC measured in the Mexican lakes may correspond to an older long-term DOC reservoir, these DOC  
758 fractions are consistent with extremely high phytoplankton release rates.

759 An interesting feature is that DOC peaks associated with primary production (mainly photosynthesis) are  
760 characterized by very positive  $\Delta^{13}\text{C}_{\text{DOC-POC}}$  (from +3 to +18 ‰, Fig. 6b). It should be noticed that a switch from  
761  $\text{CO}_{2(\text{aq})}$  to  $\text{HCO}_3^-$  as an inorganic C source (and their 10 ‰ isotopic difference, e.g. Mook et al., 1974) could not  
762 explain alone the isotopic difference between POC and DOC. The isotopic enrichment of DOC molecules  
763 compared to POC could have different origins. First, it supports that DOC may correspond to new photosynthate  
764 release rather than a product of cell lysis or zooplankton sloppy feeding, since the latter would likely produce  
765  $\delta^{13}\text{C}_{\text{DOC}}$  close to  $\delta^{13}\text{C}_{\text{POC}}$  values. Second, this heavy DOC could originate from photosynthetic organisms using a  
766 different C-fixation pathway inducing smaller isotopic fractionation. In lakes Atexcac and La Alberca anoxygenic  
767 phototrophic bacteria, and notably GSB, could release important amounts of DOC, especially under nutrient-  
768 limiting conditions (Ivanovsky et al., 2020). In contrary to PSB (another group of anoxygenic phototrophs) or  
769 cyanobacteria which use the CCB pathway, GSB use the reductive citric acid cycle or reverse tricarboxylic-TCA  
770 cycle, which tends to induce smaller isotopic fractionations (between ~ 3-13 ‰, Hayes, 2001). If the DOC  
771 reservoirs in lakes Atexcac and La Alberca's hypolimnion originate from GSB fixed C, then their isotopic  
772 composition ( $\epsilon_{\text{DOC-CO}_2} \approx -5 \pm 5$  and  $\epsilon_{\text{DOC-CO}_2} \approx -13$  ‰, respectively) are in good agreement with fractionations found  
773 for this type of organisms in laboratory cultures and other stratified water bodies (Posth et al., 2017). The DOC  
774 and POC signatures would deviate from each other if GSB only marginally participated to the POC reservoir but  
775 released most of the DOC. Third, phytoplankton blooms could specifically release isotopically heavy organic  
776 molecules. For example, carbohydrates could be preferentially released under nutrient-limiting conditions as they  
777 are devoid of N and P (Bertilsson and Jones, 2003; Wetz and Wheeler, 2007; Thornton, 2014). Carbohydrates  
778 typically have  $^{13}\text{C}$ -enriched (heavy) isotopic composition (Blair et al., 1985; Jiao et al., 2010; Close and Henderson,  
779 2020). Yet, this molecular hypothesis would hardly explain the full range of  $\Delta^{13}\text{C}_{\text{DOC-POC}}$  variations measured in  
780 Atexcac and La Alberca according to isotopic mass balance of cell specific organic compounds (Hayes, 2001). At  
781 last, such enrichments require otherwise that DOC and DIC first accumulate in the cells. Indeed, if DOC molecules  
782 were released as soon as they were produced, their isotopic composition should approach that of the biomass (i.e.  
783  $\delta^{13}\text{C}_{\text{POC}}$ , within the range of molecules-specific isotopic compositions), which is not the case. If DIC could freely  
784 exchange between inner and outer cell media, maximum "carboxylation-limited" fractionation (mostly between ~



785 18 and 30 ‰ depending on RuBisCO form, Thomas et al., 2019) would be **expressed** in all synthesized organic  
786 molecules as represented in Fig. 7a (e.g. O’Leary, 1988; Descolas-Gros and Fontungne, 1990; Fry, 1996), which  
787 is also not what DOC records (see  $\epsilon_{\text{DOC-CO}_2}$  in Fig. 6d).

788 Under the environmental conditions of the studied lakes, i.e., low  $\text{CO}_2$  quantities relative to  $\text{HCO}_3^-$ , local planktonic  
789 competition for  $\text{CO}_2$  and low nutrient availability, the activation of intracellular DIC concentrating mechanism  
790 (DIC-CM) is expected (Beardall et al., 1982; Burns and Beardall, 1987; Fogel and Cifuentes, 1993; Badger et al.,  
791 1998; Iñiguez et al., 2020). This mechanism is particularly relevant in oligotrophic aqueous media (Beardall et al.,  
792 1982), where  $\text{CO}_2$  diffusion is slower than in the air (O’Leary, 1988; Fogel and Cifuentes, 1993; Iñiguez et al.,  
793 2020). DIC-CM have been proposed to reduce the efflux of DIC from the cells back to the extracellular solution.  
794 This internal DIC is eventually converted into organic biomass, thereby drawing the cells isotopic composition  
795 closer to that of  $\delta^{13}\text{C}_{\text{DIC}}$  (Fig. 7; Beardall et al., 1982; Fogel and Cifuentes, 1993; Werne and Hollander, 2004).  
796 However, we suggest that the activation of a DIC-CM could preserve a large  $\Delta^{13}\text{C}_{\text{POC-DIC}}$  while generating an  
797 apparent fractionation between the DOC and POC molecules instead. Indeed, initially fixed OC would be  
798 discriminated against the heavy C isotopes and incorporated into the cellular biomass (Fig. 7c, ‘ $t_i$ ’). Further,  
799 following the overflow mechanism scenario, high photosynthetic rates (due to high irradiance, temperature and  
800 high DIC despite low  $\text{CO}_2$ ) coupled with low population growth rates and organic molecules synthesis (due to  
801 limited abundances of P, N, Fe, etc.) would result in the exudation of excess organic molecules with heavy  $\delta^{13}\text{C}_{\text{DOC}}$   
802 as they are synthesized from residual internal DIC, which progressively becomes  $^{13}\text{C}$ -enriched (Fig. 7c, ‘ $t_{ii}$ ’). This  
803 suggests that oligotrophic conditions could be a determinant factor in the generation of significantly heavy  
804  $\delta^{13}\text{C}_{\text{DOC}}$ , and even more if they are coupled to high irradiance.

#### 805 *DOM accumulation in Lake Alchichica*

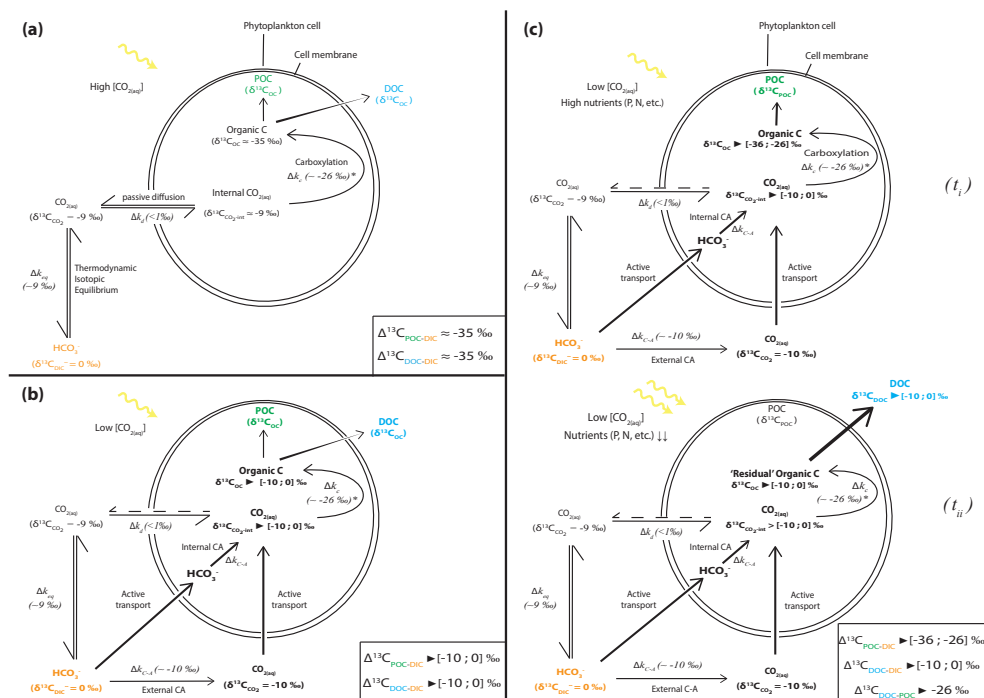
806 From the previous discussion, it appears that environmental conditions of the Mexican lakes might favor an  
807 important phytoplanktonic production of DOM. Alcocer et al. (2014) also proposed that an early spring  
808 cyanobacterial bloom in Lake Alchichica favored the production of DOC in the epilimnion. However, at the time  
809 of sampling, the DOC reservoir in this lake was not correlated with any sizeable autotrophic activity at any depth.  
810 Indeed, the large epilimnetic chlorophyll a peak did not correlate with any changes of [DOC] nor  $\delta^{13}\text{C}_{\text{DOC}}$  (Figs.  
811 2-4). Compared with the other lakes, the geochemical conditions at which chlorophyll a is produced in Alchichica  
812 could have been incompatible with the activation of a DIC-CM and significant DOM exudation. For example,  
813 Alchichica had similar  $[\text{CO}_{2(\text{aq})}]$  as La Preciosa, but higher P and  $\text{NH}_4^+$  concentrations (Table S1, S3); Lake La  
814 Alberca had higher P concentrations, but presented similar  $[\text{NH}_4^+]$  and lower  $[\text{CO}_{2(\text{aq})}]$ . We measure a large DOC  
815 increase in the middle of the anoxic hypolimnion of Lake Alchichica, but it did not correspond to any change in  
816 the DIC reservoir as observed for lakes La Preciosa (at 12.5 m) or Atexcac (at 23 m). Moreover at these depths,  
817 photosynthetic active radiation (PAR) is below 0.1% in Alchichica during the stratified season (Macek et al.,  
818 2020), which might not be sufficient to trigger important anoxygenic phytoplankton DOC release.

819 The DOC reservoir in Alchichica is characterized by a  $\delta^{13}\text{C}_{\text{DOC}}$  (and  $\Delta^{13}\text{C}_{\text{DOC-DIC}}$ ) lower than in the other lakes and  
820 systematically showing  $^{13}\text{C}$ -depleted signatures relative to POC (i.e.  $\delta^{13}\text{C}_{\text{DOC}} < \delta^{13}\text{C}_{\text{POC}}$ ; Fig. 6e). Thus, if the DOC  
821 increase in Alchichica’s hypolimnion resulted from the release of photosynthetic OC like in the other lakes, it was



822 not associated to the same C isotopes fractionation (e.g. if anoxygenic phototrophs did not actively take up DIC,  
 823 Fig. 7a).

824



825

826

827 Figure 7. Schematic view of phytoplankton cells during autotrophic C fixation through different C supply  
 828 strategies and associated apparent isotopic fractionation between DIC and POC/DOC and between DOC and POC  
 829 (cf. Table 3). (a) Case where [CO<sub>2(aq)</sub>] is high enough to allow for a DIC supply by passive CO<sub>2(aq)</sub> diffusion through  
 830 the cell membrane and CO<sub>2(aq)</sub> is at equilibrium with other DIC species. There, isotopic fractionation is maximum  
 831 (minimum δ<sup>13</sup>C<sub>OC</sub>) because C fixation is limited by the carboxylation step. DOC is released following an in- to  
 832 outward cell concentration gradient and has a similar composition to POC. (b) “Classic” view of C isotopic cycling  
 833 resulting from active DIC transport within the cell because of low ambient [CO<sub>2(aq)</sub>] (through a DIC-CM). Carbonic  
 834 anhydrase (CA) catalyzes the conversion between HCO<sub>3</sub><sup>-</sup> and CO<sub>2(aq)</sub> inside or outside the cell with an isotopic  
 835 fractionation close to equilibrium fractionation (~ 10 ‰). While inward passive CO<sub>2(aq)</sub> diffusion can still occur,  
 836 the DIC-CM activation reduces the reverse diffusion, resulting in internal CO<sub>2(aq)</sub> isotopic composition  
 837 approaching that of the incoming DIC (depending on the fraction of internal CO<sub>2(aq)</sub> leaving the cell). Acting as a  
 838 “closed-system”, most of internal DIC is fixed as OC and minimum isotopic fractionation is expressed for both  
 839 POC and DOC. (c) Proposed model for C isotopic fractionation with active DIC transport including an isotopic  
 840 discrimination between POC and DOC. (I<sub>i</sub>) Initially fixed C is isotopically depleted and incorporates the cell’s  
 841 biomass as long as there are sufficient nutrients to enable “complex” organic molecules synthesis. (I<sub>ii</sub>) In low  
 842 nutrient conditions, but high photosynthetic activity – fixed OC is released out of the cell as DOC following the  
 843 “overflow” hypothesis and inherits heavier isotopic compositions from the residual internal DIC. This leads to  
 844 distinct POC and DOC isotopic signatures, with small fractionation between DOC and DIC, the amplitude of which  
 845 will depend notably on the rate of CO<sub>2</sub> backward diffusion and ratio of biomass C (POC) and released C (DOC).



846 Alternatively, this hypolimnetic DOC increase could reflect the preservation and accumulation of DOM over the  
847 years in Lake Alchichica, consistently with higher [DOC] measured in 2019 than in the previous years (Alcocer  
848 et al., 2014). While alteration of the DOM reservoir by UV-photolysis would induce a positive isotopic  
849 fractionation (Chomicki, 2009), the slightly negative  $\Delta^{13}\text{C}_{\text{DOC-POC}}$  signatures give support to DOC being mainly a  
850 recalcitrant residual product of primary OM degradation by heterotrophic organisms (Alcocer et al., 2014). Indeed,  
851 the preferential consumption of labile  $^{13}\text{C}$ -enriched molecules by heterotrophic bacteria would leave the residual  
852 OM with more negative isotopic signatures (Sect. 5.2.2.). Moreover, degradation by heterotrophic bacteria leaves  
853 more recalcitrant DOM in the water column which tends to accumulate over longer periods of time (Ogawa et al.,  
854 2001; Jiao et al., 2010; Kawasaki et al., 2013). DOM content is a balance between its production by autotrophs  
855 and consumption by heterotrophs, especially in environments where both types of organisms compete for nutrients  
856 at a low content (Dittmar, 2015). If Alchichica's DOC actually represents a long-term reservoir, its presence might  
857 favor the development of bacterial populations growing on it. Alcocer et al. (2014) describe the shift of the  
858 cyanobacterial DOC towards the hypolimnion of Lake Alchichica at the end of the spring. Deeper and darker  
859 anoxic waters in Alchichica could better preserve DOM from intense microbial and light degradation, hence  
860 allowing its accumulation.

861 In conclusion, Alchichica's DOC reservoir (and notably in the hypolimnion) more likely represents an older and  
862 evolved DOM pool. The time required for its accumulation and its stability over the years remain to be  
863 investigated. Nevertheless, we cannot fully rule out that part of it this DOC was produced by anoxygenic  
864 photosynthetic plankton. If so, the reasons why it did not bear the same isotopic enrichment as in the other lakes  
865 also remain to be elucidated.

866

### 867 **5.3.2. DOC analysis provides deeper insights into planktonic cells functioning and water column C cycle** 868 **dynamics**

869 With concentrations ranging from 0.6 and 6.5 mM on average, DOC amounts between 14 and 160 times the POC  
870 concentrations. It represents from about 5 to 16% of total C measured in the four lakes. In comparison, although  
871 DOC is the main organic pool in the ocean, its concentration hardly exceeds 0.08 mM (Hansell, 2013) while in  
872 large scale anoxic basin such as the Black Sea, it remains under 0.3 mM (Ducklow et al., 2007). Hence DOC is a  
873 major C reservoir in these Mexican lakes.

874 The depth profiles of DOC concentration and isotopic composition differ significantly from those of POC. Notably  
875 in Lake La Preciosa, the photosynthetic DOC production (+1.5 mM) at the Chl. a peak depth matches the decrease  
876 of DIC (- 2 mM) (Fig. 3) with no change in [POC] or  $\delta^{13}\text{C}_{\text{POC}}$ . Just below, at a 15 m depth, the marked increase of  
877  $\delta^{13}\text{C}_{\text{POC}}$  related with heterotrophic activity (Sect. 0) might be better understood when considering the heavier DOC  
878 isotopes compositions as a C source between 12.5 and 15 m depth (Fig. 4). In Lake La Alberca, only a small  
879 portion of C is transferred from the inorganic to the POC by primary productivity, while the DIC reservoir is  
880 largely dominated by methanogenesis and possible volcanic degassing in the bottom of the lake. In Lake Atexcac,  
881 anoxygenic photosynthesis clearly stands out based on [DOC] and  $\delta^{13}\text{C}_{\text{DOC}}$  data, but is not recorded by the POC  
882 reservoir and only slightly by the DIC reservoir. Overall, it implies that recently fixed OC is quickly released out  
883 of the cells as DOM, thereby transferring most of C from DIC to DOC, rather than POC which, therefore, is an



884 incomplete archive of the biogeochemical reactions occurring in water columns. Furthermore, this shows that the  
885 isotopic analysis of DIC and by extension authigenic carbonates, especially in alkaline-buffered waters, might not  
886 be sensitive enough to faithfully archive environmental and biological changes.

887 The heavy  $\delta^{13}\text{C}_{\text{DOC}}$  recorded in lakes La Preciosa, La Alberca and Atexcac provides important constraints on the  
888 way planktonic cells deal with and cycle C: it may arise from the activation of a DIC-CM or from a specific  
889 metabolism or C fixation pathway. By contrast, the use of a DIC-CM is poorly captured by  $\delta^{13}\text{C}_{\text{POC}}$  analyses,  
890 although recognition of active DIC uptake has often been based on this signal (by reduced isotopic fractionation  
891 with the DIC; e.g. Beardall et al., 1982; Erez et al., 1998; Riebesell et al., 2000). Most interestingly, intra-cellular  
892 amorphous Ca-carbonates (iACC) are formed in some of the cyanobacteria from Alchichica microbialites, possibly  
893 due to supersaturated intra-cell media following active DIC uptake through a DIC-CM (Couradeau et al., 2012;  
894 Benzerara et al., 2014). While this link is still debated (Benzerara et al., 2014), the active use of DIC-CMs in the  
895 studied Mexican lakes is independently supported by the DOC isotopic signature.

896 The report that DOC is a major C reservoir in lakes has several other implications. First, the fact that a major  
897 fraction of primary and secondary productivity may be released and cycled as DOM instead of POM contrasts  
898 with the conventional view that autochthonous SOM strictly records water columns biological processes. Then, if  
899 a larger fraction of DOC incorporated the POM (e.g. due to higher nutrient availability), which later deposits as  
900 SOM, it may tend to shift both POM and SOM isotopic compositions towards higher values (e.g. Fig. 7b vs 7c).  
901 However, we notice that  $\delta^{13}\text{C}_{\text{SOC}}$  does not seem to keep track of peculiar DOC isotopic signatures, although OC  
902 carbon of the lakes is by far dominated by DOC over POC. Finally, in lakes such as Lake La Alberca, where  
903 alkalinity is not high enough to have a high buffering effect, production or consumption of DOC should increase  
904 or decrease, respectively, the  $\delta^{13}\text{C}$  of the residual lake DIC and ultimately the isotopic signatures of authigenic  
905 carbonates accumulated in the sediments (see below).

906

### 907 **5.3.3. Implications for the inference of past big DOC reservoirs**

908 The studied Mexican lakes have large DOC pools, allowing to draw comparisons with studies that have invoked  
909 past occurrences of oceanic carbon cycles dominated by big DOC reservoirs (e.g. Rothman et al., 2003; Sexton et  
910 al., 2011). Ventilation/oxidation cycles of a large deep ocean DOC reservoir have been inferred to explain  
911 carbonate isotopic records of successive warming events through the Eocene (Sexton et al., 2011). Briefly, the  
912 release of carbon dioxide into the ocean/atmosphere system following DOC oxidation would generate both the  
913 precipitation of low  $\delta^{13}\text{C}$  carbonates and an increase of the atmospheric greenhouse gas content. It was assessed  
914 that the size of this DOC reservoir should have been at least 1600 PgC (about twice the size of the modern ocean  
915 DOC reservoir) to account for a 2-4°C increase of deep ocean temperatures (Sexton et al., 2011). However, the  
916 main counter argument to this hypothesis is that the buildup of such a DOC reservoir at modern DOC production  
917 rates implies a sustained deep ocean anoxia over hundreds of thousand years, while independent geochemical  
918 proxies do not suggest such a sustained anoxia during this time interval (Rigwell and Arndt, 2015). However, our  
919 study suggests that this counter argument may be weak. Indeed, in the studied Mexican lakes, the lowest recorded  
920 [DOC] is 260  $\mu\text{M}$  (Table 1), i.e., about 6 times the deep modern ocean concentrations ( $\sim 45 \mu\text{M}$ ; Hansell, 2013).  
921 Yet, the entire water columns of these lakes down to the surficial sediments are seasonally mixed with oxygen



922 showing that high [DOC] (notably in Alchichica which likely harbor a “long-term” DOC reservoir) can be  
923 achieved despite frequent oxidative (oxygen-rich) conditions. Besides, the oxidation of only half of the DOC in  
924 the studied lakes would generate average  $\delta^{13}\text{C}_{\text{DIC}}$  deviations between -0.6 and -1 ‰, corresponding to the C  
925 isotopes excursion magnitudes described by Sexton et al. (2011).

926 Similarly, Black Sea’s deep anoxic waters hold about 3 times the amount of DOC found in the modern deep open  
927 ocean (Sexton et al., 2011; Dittmar, 2015). In the Black Sea and Mexican lakes, the low nutrient availability may  
928 limit sulfate-reduction despite high sulfate and labile organic matter concentrations, thence favoring DOM  
929 preservation and accumulation (Dittmar, 2015 and references therein). Margolin et al. (2016) argued that important  
930 DOM was only sustained by important terrigenous inputs. Our study attests the possibility for “autochthonous  
931 systems” to reach DOC concentrations well above what is found in the Black Sea and that terrigenous inputs are  
932 not needed for that. Therefore, it can be argued that the buildup of a large DOC reservoir which may have  
933 influenced the carbonates isotopic record of Eocene warming events is plausible.

934 The presence of a large oceanic DOC reservoir has also been used to account for the Neoproterozoic C isotopic  
935 record, where carbonates show  $\delta^{13}\text{C}$  negative excursions of more than 10 ‰ over tens of Ma, while paired  
936 sedimentary organic carbon isotope signal remain stable (Rothman et al., 2003; Fike et al., 2006; Swanson-Hysell  
937 et al., 2010; Tziperman et al., 2011). However, once again, this hypothesis has been questioned because of the too  
938 high DOC reservoir’s size (10 times the contemporaneous DIC, i.e.,  $10^2$  to  $10^3$  times that of modern DOC) and  
939 amount of oxidants required to generate such a sustained DOC oxidation excursion (see Ridgwell and Arndt,  
940 2015). Modeling approaches have both supported or contradicted this hypothesis: some suggested that partial  
941 oxidation of a large DOC reservoir would suffice to explain such excursions (Shi et al., 2017), while others  
942 concluded that DOC abundance in the past Earth’s oceans could not have significantly departed from today’s  
943 values (Fakraee et al., 2021). Critically, although multiple studies have built on the Neoproterozoic big DOC  
944 scenario (e.g. Li et al., 2017; Canadas et al., 2022), there is at the moment no evidence – to the best of our  
945 knowledge – for the existence of such high oceanic DOC levels in the past or present days. Modern analogous  
946 systems such as the Black Sea or Mexican lakes studied here support the possibility of important DOC contents  
947 accumulation but those remain substantially lower than the levels required to account for the Neoproterozoic events  
948 (Ducklow et al., 2007; Ridgwell and Arndt, 2015).

949 In the studied lakes, a full DOC oxidation would generate a maximum  $\delta^{13}\text{C}_{\text{DIC}}$  deviation of -2 ‰, in Alberca de  
950 los Espinos, which has the lowest alkalinity, and the lowest  $\delta^{13}\text{C}_{\text{DIC}}$ . The other lakes  $\delta^{13}\text{C}_{\text{DIC}}$  are less impacted,  
951 notably because they are largely buffered by high DIC content (Table 1). Bade et al. (2004) showed that low  
952 alkalinity/low pH lakes generally show more negative  $\delta^{13}\text{C}_{\text{DIC}}$  (down to ~ -30‰), partly due to a higher response  
953 to remineralization of OM and especially DOC. Compiling our data with those of Bade et al. (2004) we consistently  
954 show a clear negative trend of  $\delta^{13}\text{C}_{\text{DIC}}$  with increasing DOC:DIC ratio over a broad range of lacustrine DOC and  
955 DIC concentrations (Fig. S3a). This observation is consistent with the inference that systems where  $\text{DOC:DIC} \gg$   
956 1 should drive  $\delta^{13}\text{C}_{\text{DIC}}$  to very negative values (Rothman et al., 2003). In high DOC:DIC environments, the biomass  
957 is largely influenced by heterotrophs and usually lean towards acidic pHs (Fig. S3b; Bade et al., 2004). Hence,  
958 environmental conditions where  $\text{DOC:DIC} \gg 1$  might be inconsistent with large carbonate deposits. Accordingly,  
959 in light of the present results, Neoproterozoic carbonate carbon isotope excursions seem unlikely to be explained  
960 by the big DOC scenario, unless DOC and DIC pools are spatially decoupled (e.g. through terrestrial DOM inputs).



961 **6. CONCLUSIONS AND SUMMARY**

962 The carbon cycle of four stratified alkaline crater lakes were described and extensively compared, including the  
963 concentration and isotopic compositions of DIC, DOC, POC and surficial (~10 cm) sedimentary carbonates and  
964 organic carbon (SOC) in parallel with their physico-chemical characteristics. We identify different regimes of C  
965 cycling in the four lakes due to different biogeochemical reactions related to slight environmental and ecological  
966 changes. In more details, we show that:

- 967 - external abiotic factors such as the hydrological regime and the inorganic C sources to the lakes control  
968 their alkalinity and thus, the buffering capacities of their waters. In turn, it constrains the stratification of  
969 the water columns and thus the distribution of microbial communities and their respective metabolic  
970 effect on C.
- 971 - Based on POC and DIC concentrations and isotopic compositions, coupled with physico-chemical  
972 parameters, we are able to identify the activity of oxygenic photosynthesis and aerobic respiration in the  
973 four studied lakes. Anoxygenic photosynthesis and/or chemoautotrophy as well as sediment-related  
974 methanogenesis are also evidenced in some of the lakes, but their POC and DIC signatures can be  
975 equivocal.
- 976 - DOC is the largest OC reservoir in the water column of the studied lakes (> 90%). Its concentrations and  
977 isotopic compositions bring precious new and complementary information about the C cycle of these  
978 stratified water bodies. Depending on environmental factors such as nutrients and DIC availability,  
979 diverse photosynthetic planktonic communities appear to release more or less important amounts of DOC  
980 depending on the lake, transferring most of the inorganic C fixed to DOC rather than POC. This process  
981 is marked by very heavy and distinct isotopic signatures of DOC compared to POC. They reflect different  
982 metabolism/C fixation pathways and/or the activity of a DIC-CM coupled with an overflow mechanism  
983 (i.e. DOM exudation) for which we propose a novel isotopic model including DOC. These features are  
984 invisible to POC analyses and thus are not recorded in the sediments.
- 985 - Our results bring further constraints on the environmental conditions in which autochthonous DOM can  
986 accumulate in anoxic water bodies and provides boundary conditions to the “big DOC reservoir” scenario.
- 987 - We observe that the SOM geochemical signatures of these stratified lakes do not all record the same  
988 biogeochemical layers of the water column and can be largely modified by early diagenesis in some cases.
- 989 - Methanogenesis is evidenced in the surficial sediments of the organic-rich Lake La Alberca de los Espinos  
990 and influences the lower water column geochemical signatures. However, it is recorded only by analyses  
991 of pore water dissolved species and not in its sedimentary archives (OM and carbonates).

992

993 **Author Contributions**

994 RH and CT designed the study in a project directed by PLG, KB and CT. CT, MI, DJ, DM, RT, PLG and KB  
995 collected the samples on the field. RH carried out the measurements for C data; DJ the physico-chemical parameter  
996 probe measurements and EM provided data for trace and major elements. RH and CT analyzed the data. RH wrote  
997 the manuscript with important contributions of all co-authors.

998



999 **Competing Interests**

1000 The authors declare that they have no conflict of interest.

1001

1002 **Disclaimer**

1003

1004 **Acknowledgements**

1005 This work was supported by Agence Nationale de la Recherche (France; ANR Microbialites, grant number ANR-  
1006 18-CE02-0013-02). The authors thank Anne-Lise Santoni, Elodie Cognard, Théophile Cocquerez and the GISMO  
1007 platform (Biogéosciences, University Bourgogne Franche-Comté, UMR CNRS 6282, France). We thank Céline  
1008 Liorzou and Bleuenn Guéguen for the analyses at the Pôle Spectrométrie Océan (Laboratoire Géo-Océan, Brest,  
1009 France) and Laure Cordier for ion chromatography analyses at IPGP (France). We thank Nelly Assayag and Pierre  
1010 Cadeau for their help on the AP 2003 at IPGP.

1011

1012 **References**

- 1013 Adame, M.F., Alcocer, J., Escobar, E.: Size-fractionated phytoplankton biomass and its implications for the  
1014 dynamics of an oligotrophic tropical lake. *Freshw. Biol.* 53, 22–31. [https://doi.org/10.1111/j.1365-  
1015 2427.2007.01864.x](https://doi.org/10.1111/j.1365-2427.2007.01864.x), 2008.
- 1016 Alcocer, J.: Lake Alchichica Limnology, Springer Nature. ed. [https://link.springer.com/book/10.1007/978-3-  
1017 030-79096-7](https://link.springer.com/book/10.1007/978-3-030-79096-7), 2021.
- 1018 Alcocer, J., Guzmán-Arias, A., Oseguera, L.A., Escobar, E.: Dinámica del carbono orgánico disuelto y  
1019 particulado asociados al florecimiento de *Nodularia spumigena* en un lago tropical oligotrófico. *Programma*  
1020 *Mex. Carbono* 13, 2014.
- 1021 Anderson, N.John., Stedmon, C.A.: The effect of evapoconcentration on dissolved organic carbon concentration  
1022 and quality in lakes of SW Greenland. *Freshw. Biol.* 52, 280–289. [https://doi.org/10.1111/j.1365-  
1023 2427.2006.01688.x](https://doi.org/10.1111/j.1365-2427.2006.01688.x), 2007.
- 1024 Armienta, M.A., Vilaclara, G., De la Cruz-Reyna, S., Ramos, S., Cenicerros, N., Cruz, O., Aguayo, A., Arcega-  
1025 Cabrera, F.: Water chemistry of lakes related to active and inactive Mexican volcanoes. *J. Volcanol. Geotherm.*  
1026 *Res.* 178, 249–258. <https://doi.org/10.1016/j.jvolgeores.2008.06.019>, 2008.
- 1027 Armstrong-Altrin, J.S., Madhavaraju, J., Sial, A.N., Kasper-Zubillaga, J.J., Nagarajan, R., Flores-Castro, K.,  
1028 Rodríguez, J.L.: Petrography and stable isotope geochemistry of the cretaceous El Abra Limestones (Actopan),  
1029 Mexico: Implication on diagenesis. *J. Geol. Soc. India* 77, 349–359. <https://doi.org/10.1007/s12594-011-0042-3>,  
1030 2011.
- 1031 Assayag, N., Jézéquel, D., Ader, M., Viollier, E., Michard, G., Prévot, F., Agrinier, P.: Hydrological budget,  
1032 carbon sources and biogeochemical processes in Lac Pavin (France): Constraints from  $\delta^{18}\text{O}$  of water and  $\delta^{13}\text{C}$   
1033 of dissolved inorganic carbon. *Appl. Geochem.* 23, 2800–2816.  
1034 <https://doi.org/10.1016/j.apgeochem.2008.04.015>, 2008.
- 1035 Assayag, N., Rivé, K., Ader, M., Jézéquel, D., Agrinier, P.: Improved method for isotopic and quantitative  
1036 analysis of dissolved inorganic carbon in natural water samples. *Rapid Commun. Mass Spectrom.* 20, 2243–  
1037 2251. <https://doi.org/10.1002/rcm.2585>, 2006.
- 1038 Bade, D.L., Carpenter, S.R., Cole, J.J., Hanson, P.C., Hesslein, R.H.: Controls of  $\delta^{13}\text{C}$ -DIC in lakes:  
1039 Geochemistry, lake metabolism, and morphometry. *Limnol. Oceanogr.* 49, 1160–1172.  
1040 <https://doi.org/10.4319/lo.2004.49.4.1160>, 2004.



- 1041 Bade, D.L., Carpenter, S.R., Cole, J.J., Pace, M.L., Kritzberg, E., Van de Bogert, M.C., Cory, R.M., McKnight,  
1042 D.M.: Sources and fates of dissolved organic carbon in lakes as determined by whole-lake carbon isotope  
1043 additions. *Biogeochemistry* 84, 115–129. <https://doi.org/10.1007/s10533-006-9013-y>, 2007.
- 1044 Badger, M.R., Andrews, T.J., Whitney, S.M., Ludwig, M., Yellowlees, D.C., Leggat, W. and Price, G.D.: The  
1045 diversity and coevolution of Rubisco, plastids, pyrenoids, and chloroplast-based CO<sub>2</sub>-concentrating mechanisms  
1046 in algae. *Canadian Journal of Botany*, 76(6), pp.1052-1071, <https://doi.org/10.1139/b98-074>, 1998.
- 1047 Baines, S.B., Pace, M.L.: The production of dissolved organic matter by phytoplankton and its importance to  
1048 bacteria: Patterns across marine and freshwater systems. *Limnol. Oceanogr.* 36, 1078–1090.  
1049 <https://doi.org/10.4319/lo.1991.36.6.1078>, 1991.
- 1050 Beardall, J., Griffiths, H., Raven, J.A.: Carbon Isotope Discrimination and the CO<sub>2</sub> Accumulating Mechanism in  
1051 *Chlorella emersonii*. *J. of Expe. Botany*, 33, 729–737. <https://doi.org/10.1093/jxb/33.4.729>, 1982.
- 1052 Beaupré, S.R.: The Carbon Isotopic Composition of Marine DOC, in: *Biogeochemistry of Marine Dissolved*  
1053 *Organic Matter*. Elsevier, pp. 335–368. <https://doi.org/10.1016/B978-0-12-405940-5.00006-6>, 2015.
- 1054 Bekker, A., Holmden, C., Beukes, N.J., Kenig, F., Eglinton, B., Patterson, W.P.: Fractionation between inorganic  
1055 and organic carbon during the Lomagundi (2.22–2.1 Ga) carbon isotope excursion. *Earth Planet. Sci. Lett.* 271,  
1056 278–291. <https://doi.org/10.1016/j.epsl.2008.04.021>, 2008.
- 1057 Benzerara, K., Skouri-Panet, F., Li, J., Féraud, C., Gugger, M., Laurent, T., Couradeau, E., Ragon, M., Cosmidis,  
1058 J., Menguy, N., Margaret-Oliver, I., Tavera, R., López-García, P., Moreira, D.: Intracellular Ca-carbonate  
1059 biomineralization is widespread in cyanobacteria. *Proc. Natl. Acad. Sci.* 111, 10933–10938.  
1060 <https://doi.org/10.1073/pnas.1403510111>, 2014.
- 1061 Bertilsson, S., Jones, J.B.: Supply of Dissolved Organic Matter to Aquatic Ecosystems: Autochthonous Sources,  
1062 in: Findlay, S.E.G., Sinsabaugh, R.L. (Eds.), *Aquatic Ecosystems, Aquatic Ecology*. Academic Press,  
1063 Burlington, pp. 3–24. <https://doi.org/10.1016/B978-012256371-3/50002-0>, 2003.
- 1064 Birgel, D., Meister, P., Lundberg, R., Horath, T.D., Bontognali, T.R.R., Bahniuk, A.M., de Rezende, C.E.,  
1065 Vasconcelos, C., McKenzie, J.A.: Methanogenesis produces strong <sup>13</sup>C enrichment in stromatolites of Lagoa  
1066 Salgada, Brazil: a modern analogue for Palaeo-/Neoproterozoic stromatolites? *Geobiology* 13, 245–266.  
1067 <https://doi.org/10.1111/gbi.12130>, 2015.
- 1068 Blair, N., Leu, A., Muñoz, E., Olsen, J., Kwong, E., Des Marais, D.: Carbon isotopic fractionation in  
1069 heterotrophic microbial metabolism. *Appl. Environ. Microbiol.* 50, 996–1001.  
1070 <https://doi.org/10.1128/aem.50.4.996-1001.1985>, 1985.
- 1071 Brailsford, F.L.: *Dissolved organic matter (DOM) in freshwater ecosystems*. Bangor University (UK), 2019
- 1072 Briones, E.E., Alcocer, J., Cienfuegos, E., Morales, P.: Carbon stable isotopes ratios of pelagic and littoral  
1073 communities in Alchichica crater-lake, Mexico. *Int. J. Salt Lake Res.* 7, 345–355.  
1074 <https://doi.org/10.1007/BF02442143>, 1998.
- 1075 Buchan, A., LeClerc, G.R., Gulvik, C.A., González, J.M.: Master recyclers: features and functions of bacteria  
1076 associated with phytoplankton blooms. *Nat. Rev. Microbiol.* 12, 686–698. <https://doi.org/10.1038/nrmicro3326>,  
1077 2014.
- 1078 Burns, B.D., Beardall, J.: Utilization of inorganic carbon by marine microalgae. *J. Exp. Mar. Biol. Ecol.* 107,  
1079 75–86. [https://doi.org/10.1016/0022-0981\(87\)90125-0](https://doi.org/10.1016/0022-0981(87)90125-0), 1987.
- 1080 Cadeau, P., Jézéquel, D., Lebourlangier, C., Fouilland, E., Le Floc’h, E., Chaduteau, C., Milesi, V., Guélard, J.,  
1081 Sarazin, G., Katz, A., d’Amore, S., Bernard, C., Ader, M.: Carbon isotope evidence for large methane emissions  
1082 to the Proterozoic atmosphere. *Sci. Rep.* 10, 18186. <https://doi.org/10.1038/s41598-020-75100-x>, 2020.
- 1083 Cai, C., Li, K., Liu, D., John, C.M., Wang, D., Fu, B., Fakhraee, M., He, H., Feng, L., Jiang, L.: Anaerobic  
1084 oxidation of methane by Mn oxides in sulfate-poor environments. *Geology* 49, 761–766.  
1085 <https://doi.org/10.1130/G48553.1>, 2021.



- 1086 Callieri, C., Coci, M., Corno, G., Macek, M., Modenutti, B., Balseiro, E., Bertoni, R.: Phylogenetic diversity of  
1087 nonmarine picocyanobacteria. *FEMS Microbiol. Ecol.* 85, 293–301. <https://doi.org/10.1111/1574-6941.12118> ,  
1088 2013.
- 1089 Camacho, A., Walter, X.A., Picazo, A., Zopf, J.: Photoferrotrophy: Remains of an Ancient Photosynthesis in  
1090 Modern Environments. *Front. Microbiol.* 08. <https://doi.org/10.3389/fmicb.2017.00323> , 2017.
- 1091 Cañadas, F., Papineau, D., Leng, M.J. and Li, C.: Extensive primary production promoted the recovery of the  
1092 Ediacaran Shuram excursion. *Nature communications*, 13, 1-9. <https://doi.org/10.1038/s41467-021-27812-5> ,  
1093 2022.
- 1094 Carlson, C.A., Hansell, D.A.: DOM Sources, Sinks, Reactivity, and Budgets, in: *Biogeochemistry of Marine*  
1095 *Dissolved Organic Matter*. Elsevier, pp. 65–126. <https://doi.org/10.1016/B978-0-12-405940-5.00003-0> , 2015.
- 1096 Carrasco-Núñez, G., Ort, M.H., Romero, C.: Evolution and hydrological conditions of a maar volcano (Atexcac  
1097 crater, Eastern Mexico). *J. Volcanol. Geotherm. Res.* 159, 179–197.  
1098 <https://doi.org/10.1016/j.jvolgeores.2006.07.001> , 2007.
- 1099 Chako Tchamabé, B., Carrasco-Núñez, G., Miggins, D.P., Németh, K.: Late Pleistocene to Holocene activity of  
1100 Alchichica maar volcano, eastern Trans-Mexican Volcanic Belt. *J. South Am. Earth Sci.* 97, 102404.  
1101 <https://doi.org/10.1016/j.jsames.2019.102404> , 2020.
- 1102 Cheng, C., Zhang, J., He, Q., Wu, H., Chen, Y., Xie, H., Pavlostathis, S.G.: Exploring simultaneous nitrous  
1103 oxide and methane sink in wetland sediments under anoxic conditions. *Water Res.* 194, 116958.  
1104 <https://doi.org/10.1016/j.watres.2021.116958> , 2021.
- 1105 Chomicki, K.: The use of stable carbon and oxygen isotopes to examine the fate of dissolved organic matter in  
1106 two small, oligotrophic Canadian Shield lakes. University of Waterloo (Canada) , 2009.
- 1107 Close, H.G., Henderson, L.C.: Open-Ocean Minima in  $\delta^{13}\text{C}$  Values of Particulate Organic Carbon in the Lower  
1108 Euphotic Zone. *Front. Mar. Sci.* 7, 540165. <https://doi.org/10.3389/fmars.2020.540165> , 2020.
- 1109 Couradeau, E., Benzerara, K., Gérard, E., Moreira, D., Bernard, S., Brown, G.E., López-García, P.: An Early-  
1110 Branching Microbialite Cyanobacterium Forms Intracellular Carbonates. *Science* 336, 459–462.  
1111 <https://doi.org/10.1126/science.1216171> , 2012.
- 1112 Crowe, S.A., Katsev, S., Leslie, K., Sturm, A., Magen, C., Nomosatryo, S., Pack, M.A., Kessler, J.D., Reeburgh,  
1113 W.S., Roberts, J.A., González, L., Douglas Haffner, G., Mucci, A., Sundby, B., Fowle, D.A.: The methane cycle  
1114 in ferruginous Lake Matano: Methane cycle in ferruginous Lake Matano. *Geobiology* 9, 61–78.  
1115 <https://doi.org/10.1111/j.1472-4669.2010.00257.x> , 2011.
- 1116 Descolas-Gros, C., Fontugne, M.: Stable carbon isotope fractionation by marine phytoplankton during  
1117 photosynthesis. *Plant Cell Environ.* 13, 207–218. <https://doi.org/10.1111/j.1365-3040.1990.tb01305.x> , 1990.
- 1118 Dittmar, T.: Reasons Behind the Long-Term Stability of Dissolved Organic Matter, in: *Biogeochem. of Marine*  
1119 *Dissolved Organic Matter* (pp. 369–388). Academic Press. <https://doi.org/10.1016/B978-0-12-405940-5.00007-8>  
1120 , 2015.
- 1121 Ducklow, H.W., Hansell, D.A., Morgan, J.A.: Dissolved organic carbon and nitrogen in the Western Black Sea.  
1122 *Mar. Chem.* 105, 140–150. <https://doi.org/10.1016/j.marchem.2007.01.015> , 2007.
- 1123 Emrich, K., Ehhalt, D.H., Vogel, J.C.: Carbon isotope fractionation during the precipitation of calcium  
1124 carbonate. *Earth Planet. Sci. Lett.* 8, 363–371. [https://doi.org/10.1016/0012-821X\(70\)90109-3](https://doi.org/10.1016/0012-821X(70)90109-3) , 1970.
- 1125 Erez, J., Bouevitch, A., Kaplan, A.: Carbon isotope fractionation by photosynthetic aquatic microorganisms:  
1126 experiments with *Synechococcus* PCC7942, and a simple carbon flux model. *Can. J. Bot.* 76, 1109–1118.  
1127 <https://doi.org/10.1139/b98-067> , 1998.
- 1128 Fakhraee, M., Tarhan, L.G., Planavsky, N.J., Reinhard, C.T.: A largely invariant marine dissolved organic  
1129 carbon reservoir across Earth’s history. *Proc. Natl. Acad. Sci.* 118, e2103511118.  
1130 <https://doi.org/10.1073/pnas.2103511118> , 2021.



- 1131 Ferrari, L., Orozco-Esquivel, T., Manea, V., Manea, M.: The dynamic history of the Trans-Mexican Volcanic  
1132 Belt and the Mexico subduction zone. *Tectonophysics* 522–523, 122–149.  
1133 <https://doi.org/10.1016/j.tecto.2011.09.018> , 2012.
- 1134 Fike, D.A., Grotzinger, J.P., Pratt, L.M., Summons, R.E.: Oxidation of the Ediacaran Ocean. *Nature* 444, 744–  
1135 747. <https://doi.org/10.1038/nature05345> , 2006.
- 1136 Fogel, M.L., Cifuentes, L.A.: Isotope Fractionation during Primary Production, in: Engel, M.H., Macko, S.A.  
1137 (Eds.), *Organic Geochemistry, Topics in Geobiology*. Springer US, Boston, MA, pp. 73–98.  
1138 [https://doi.org/10.1007/978-1-4615-2890-6\\_3](https://doi.org/10.1007/978-1-4615-2890-6_3) , 1993.
- 1139 Fry, B.:  $^{13}\text{C}/^{12}\text{C}$  fractionation by marine diatoms. *Mar. Ecol. Prog. Ser.* 134, 283–294.  
1140 <https://doi.org/10.3354/meps134283> , 1996.
- 1141 Fry, B., Jannasch, H.W., Molyneux, S.J., Wirsén, C.O., Muramoto, J.A., King, S.: Stable isotope studies of the  
1142 carbon, nitrogen and sulfur cycles in the Black Sea and the Cariaco Trench. *Deep Sea Res. Part Oceanogr. Res.*  
1143 *Pap.* 38, S1003–S1019. [https://doi.org/10.1016/S0198-0149\(10\)80021-4](https://doi.org/10.1016/S0198-0149(10)80021-4) , 1991
- 1144 Fulton, J.M., Arthur, M.A., Thomas, B., Freeman, K.H.: Pigment carbon and nitrogen isotopic signatures in  
1145 euxinic basins. *Geobiology* 16, 429–445. <https://doi.org/10.1111/gbi.12285> , 2018.
- 1146 Furian, S., Martins, E.R.C., Parizotto, T.M., Rezende-Filho, A.T., Victoria, R.L., Barbiero, L.: Chemical  
1147 diversity and spatial variability in myriad lakes in Nhecolândia in the Pantanal wetlands of Brazil. *Limnol.*  
1148 *Oceanogr.* 58, 2249–2261. <https://doi.org/10.4319/lo.2013.58.6.2249> , 2013.
- 1149 Gérard, E., Ménez, B., Couradeau, E., Moreira, D., Benzerara, K., Tavera, R. and López-García, P.: Specific  
1150 carbonate–microbe interactions in the modern microbialites of Lake Alchichica (Mexico). *The ISME journal*, 7,  
1151 1997–2009. <https://doi.org/10.1038/ismej.2013.81> , 2013.
- 1152 Gröger, J., Franke, J., Hamer, K., Schulz, H.D.: Quantitative Recovery of Elemental Sulfur and Improved  
1153 Selectivity in a Chromium-Reducible Sulfur Distillation. *Geostand. Geoanalytical Res.* 33, 17–27.  
1154 <https://doi.org/10.1111/j.1751-908X.2009.00922.x> , 2009.
- 1155 Gu, B., Schelske, C.L., Hodell, D.A.: Extreme  $^{13}\text{C}$  enrichments in a shallow hypereutrophic lake: Implications  
1156 for carbon cycling. *Limnol. Oceanogr.* 49, 1152–1159. <https://doi.org/10.4319/lo.2004.49.4.1152> , 2004.
- 1157 Hansell, D.A.: Recalcitrant Dissolved Organic Carbon Fractions. *Annu. Rev. Mar. Sci.* 5, 421–445.  
1158 <https://doi.org/10.1146/annurev-marine-120710-100757> , 2013.
- 1159 Hassan, K.M.: Isotope geochemistry of Swan Lake Basin in the Nebraska Sandhills, USA: Large  $^{13}\text{C}$  enrichment  
1160 in sediment–calcite records. *Geochemistry* 74, 681–690. <https://doi.org/10.1016/j.chemer.2014.03.004> , 2014.
- 1161 Havig, J.R., Hamilton, T.L., McCormick, M., McClure, B., Sowers, T., Wegter, B., Kump, L.R.: Water column  
1162 and sediment stable carbon isotope biogeochemistry of permanently redox- stratified Fayetteville Green Lake,  
1163 New York, U.S.A. *Limnol. Oceanogr.* 63, 570–587. <https://doi.org/10.1002/lno.10649> , 2018.
- 1164 Havig, J.R., McCormick, M.L., Hamilton, T.L., Kump, L.R.: The behavior of biologically important trace  
1165 elements across the oxic/euxinic transition of meromictic Fayetteville Green Lake, New York, USA. *Geochim.*  
1166 *Cosmochim. Acta* 165, 389–406. <https://doi.org/10.1016/j.gca.2015.06.024> , 2015.
- 1167 Hayes, J.M.: Fractionation of Carbon and Hydrogen Isotopes in Biosynthetic Processes\*. *Rev. Mineral.*  
1168 *Geochem.* 43, 225–277. <https://doi.org/10.2138/gsrmg.43.1.225> , 2001.
- 1169 Hayes, J.M., Popp, B.N., Takigiku, R., Johnson, M.W.: An isotopic study of biogeochemical relationships  
1170 between carbonates and organic carbon in the Greenhorn Formation. *Geochim. Cosmochim. Acta* 53, 2961–  
1171 2972. [https://doi.org/10.1016/0016-7037\(89\)90172-5](https://doi.org/10.1016/0016-7037(89)90172-5) , 1989.
- 1172 Henkel, J.V., Dellwig, O., Pollehne, F., Herlemann, D.P.R., Leipe, T., Schulz-Vogt, H.N.: A bacterial isolate  
1173 from the Black Sea oxidizes sulfide with manganese(IV) oxide. *Proc. Natl. Acad. Sci.* 116, 12153–12155.  
1174 <https://doi.org/10.1073/pnas.1906000116> , 2019.



- 1175 Hessen, D.O.: Dissolved organic carbon in a humic lake: effects on bacterial production and respiration.  
1176 *Hydrobiologia*, 229(1), pp.115-123. [https://doi.org/10.1007/978-94-011-2474-4\\_9](https://doi.org/10.1007/978-94-011-2474-4_9), 1992.
- 1177 Hessen, D.O., Anderson, T.R.: Excess carbon in aquatic organisms and ecosystems: Physiological, ecological,  
1178 and evolutionary implications. *Limnol. Oceanogr.* 53, 1685–1696. <https://doi.org/10.4319/lo.2008.53.4.1685>,  
1179 2008.
- 1180 Iniesto, M., Moreira, D., Benzerara, K., Muller, E., Bertolino, P., Tavera, R. and López- García, P.: Rapid  
1181 formation of mature microbialites in Lake Alchichica, Mexico. *Env. Microbio. Reports*, 13, 600-605.  
1182 <https://doi.org/10.1111/1758-2229.12957>, 2021a.
- 1183 Iniesto, M., Moreira, D., Reboul, G., Deschamps, P., Benzerara, K., Bertolino, P., Saghafi, A., Tavera, R. and  
1184 López- García, P.: Core microbial communities of lacustrine microbialites sampled along an alkalinity gradient.  
1185 *Env. Microbio.*, 23, 51-68. <https://doi.org/10.1111/1462-2920.15252>, 2021b.
- 1186 Iniesto, M., Moreira, D., Benzerara, K., Reboul G., Bertolino, P., Tavera, R. and López- García, P.: Planktonic  
1187 microbial communities from microbialite-bearing lakes sampled along a salinity-alkalinity gradient. *Limnol.*  
1188 *Oceanogr.* In press.
- 1189 Iñiguez, C., Capó- Bauçà, S., Niinemets, Ü., Stoll, H., Aguiló- Nicolau, P., Galmés, J.: Evolutionary trends in  
1190 RuBisCO kinetics and their co- evolution with CO<sub>2</sub> concentrating mechanisms. *Plant J.* 101, 897–918.  
1191 <https://doi.org/10.1111/tpj.14643>, 2020.
- 1192 Ivanovsky, R.N., Lebedeva, N.V., Keppen, O.I., Chudnovskaya, A.V.: Release of Photosynthetically Fixed  
1193 Carbon as Dissolved Organic Matter by Anoxygenic Phototrophic Bacteria. *Microbiology* 89, 28–34.  
1194 <https://doi.org/10.1134/S0026261720010075>, 2020.
- 1195 Javoy, M., Pineau, F., Delorme, H.: Carbon and nitrogen isotopes in the mantle. *Chem. Geol., Isotopes in*  
1196 *Geology—Picciotto Volume* 57, 41–62. [https://doi.org/10.1016/0009-2541\(86\)90093-8](https://doi.org/10.1016/0009-2541(86)90093-8), 1986.
- 1197 Jézéquel, D., Michard, G., Viollier, E., Agrinier, P., Albéric, P., Lopes, F., Abril, G. and Bergonzini, L.: Carbon  
1198 cycle in a meromictic crater lake: Lake Pavin, France. In *Lake Pavin* (pp. 185-203). Springer, Cham.  
1199 [https://doi.org/10.1007/978-3-319-39961-4\\_11](https://doi.org/10.1007/978-3-319-39961-4_11), 2016.
- 1200 Jiao, N., Herndl, G.J., Hansell, D.A., Benner, R., Kattner, G., Wilhelm, S.W., Kirchman, D.L., Weinbauer, M.G.,  
1201 Luo, T., Chen, F., Azam, F.: Microbial production of recalcitrant dissolved organic matter: long-term carbon  
1202 storage in the global ocean. *Nat. Rev. Microbiol.* 8, 593–599. <https://doi.org/10.1038/nrmicro2386>, 2010.
- 1203 Kaplan, L.A., Wiegner, T.N., Newbold, J.D., Ostrom, P.H., Gandhi, H.: Untangling the complex issue of  
1204 dissolved organic carbon uptake: a stable isotope approach. *Freshw. Biol.* 53, 855–864.  
1205 <https://doi.org/10.1111/j.1365-2427.2007.01941.x>, 2008.
- 1206 Karhu, J.A. and Holland, H.D.: Carbon isotopes and the rise of atmospheric oxygen. *Geology* 24, 867-870,  
1207 [https://doi.org/10.1130/0091-7613\(1996\)024<0867:CIATRO>2.3.CO;2](https://doi.org/10.1130/0091-7613(1996)024<0867:CIATRO>2.3.CO;2), 1996.
- 1208 Kawasaki, N., Komatsu, K., Kohzu, A., Tomioka, N., Shinohara, R., Satou, T., Watanabe, F.N., Tada, Y.,  
1209 Hamasaki, K., Kushairi, M.R.M., Imai, A.: Bacterial Contribution to Dissolved Organic Matter in Eutrophic  
1210 Lake Kasumigaura, Japan. *Appl. Environ. Microbiol.* 79, 7160–7168. <https://doi.org/10.1128/AEM.01504-13>,  
1211 2013.
- 1212 Klawonn, I., Van den Wyngaert, S., Parada, A.E., Arandia-Gorostidi, N., Whitehouse, M.J., Grossart, H.-P.,  
1213 Dekas, A.E.: Characterizing the “fungal shunt”: Parasitic fungi on diatoms affect carbon flow and bacterial  
1214 communities in aquatic microbial food webs. *Proc. Natl. Acad. Sci.* 118, e2102225118.  
1215 <https://doi.org/10.1073/pnas.2102225118>, 2021.
- 1216 Knossow, N., Blonder, B., Eckert, W., Turchyn, A.V., Antler, G., Kamyshny, A.: Annual sulfur cycle in a warm  
1217 monomictic lake with sub-millimolar sulfate concentrations. *Geochem. Trans.* 16, 7.  
1218 <https://doi.org/10.1186/s12932-015-0021-5>, 2015.
- 1219 Kuntz, L.B., Laakso, T.A., Schrag, D.P., Crowe, S.A.: Modeling the carbon cycle in Lake Matano. *Geobiology*  
1220 13, 454–461. <https://doi.org/10.1111/gbi.12141>, 2015.



- 1221 Lampert, W.: Release of dissolved organic carbon by grazing zooplankton. *Limnol. Oceanogr.* 23, 831–834.  
1222 <https://doi.org/10.4319/lo.1978.23.4.0831>, 1978.
- 1223 Lehmann, M.F., Bernasconi, S.M., Barbieri, A., McKenzie, J.A.: Preservation of organic matter and alteration of  
1224 its carbon and nitrogen isotope composition during simulated and in situ early sedimentary diagenesis. *Geochim.*  
1225 *Cosmochim. Acta* 66, 3573–3584. [https://doi.org/10.1016/S0016-7037\(02\)00968-7](https://doi.org/10.1016/S0016-7037(02)00968-7), 2002.
- 1226 Lehmann, M.F., Bernasconi, S.M., McKenzie, J.A., Barbieri, A., Simona, M., Veronesi, M.: Seasonal variation  
1227 of the  $\delta\text{C}$  and  $\delta\text{N}$  of particulate and dissolved carbon and nitrogen in Lake Lugano: Constraints on  
1228 biogeochemical cycling in a eutrophic lake. *Limnol. Oceanogr.* 49, 415–429.  
1229 <https://doi.org/10.4319/lo.2004.49.2.0415>, 2004.
- 1230 Lelli, M., Kretzschmar, T.G., Cabassi, J., Doveri, M., Sanchez-Avila, J.I., Gherardi, F., Magro, G., Norelli, F.:  
1231 Fluid geochemistry of the Los Humeros geothermal field (LHGF - Puebla, Mexico): New constraints for the  
1232 conceptual model. *Geothermics* 90, 101983. <https://doi.org/10.1016/j.geothermics.2020.101983>, 2021.
- 1233 Li, C., Hardisty, D.S., Luo, G., Huang, J., Algeo, T.J., Cheng, M., Shi, W., An, Z., Tong, J., Xie, S. and Jiao, N.:  
1234 Uncovering the spatial heterogeneity of Ediacaran carbon cycling. *Geobio.*, 15, 211–224.  
1235 <https://doi.org/10.1111/gbi.12222>, 2017.
- 1236 Li, H.-C., Ku, T.-L.:  $\delta^{13}\text{C}$ – $\delta^{18}\text{C}$  covariance as a paleohydrological indicator for closed-basin lakes. *Palaeogeogr.*  
1237 *Palaeoclimatol. Palaeoecol.* 133, 69–80. [https://doi.org/10.1016/S0031-0182\(96\)00153-8](https://doi.org/10.1016/S0031-0182(96)00153-8), 1997.
- 1238 Lorenz, V.: On the growth of maars and diatremes and its relevance to the formation of tuff rings. *Bull.*  
1239 *Volcanol.* 48, 265–274. <https://doi.org/10.1007/BF01081755>, 1986.
- 1240 Lugo, A., Alcocer, J., Sánchez, Ma. del R., Escobar, E., Macek, M.: Temporal and spatial variation of  
1241 bacterioplankton abundance in a tropical, warm-monomictic, saline lake: Alchichica, Puebla, Mexico. *SIL Proc.*  
1242 1922–2010 27, 2968–2971. <https://doi.org/10.1080/03680770.1998.11898217>, 2000.
- 1243 Lugo, A., Alcocer, J., Sanchez, M.R., Escobar, E.: Trophic status of tropical lakes indicated by littoral protozoan  
1244 assemblages. *SIL Proc.* 1922–2010 25, 441–443. <https://doi.org/10.1080/03680770.1992.11900159>, 1993.
- 1245 Lyons, T.W., Reinhard, C.T., Planavsky, N.J.: The rise of oxygen in Earth's early ocean and atmosphere. *Nature*  
1246 506, 307–315. <https://doi.org/10.1038/nature13068>, 2014.
- 1247 Macek, M., Medina, X.S., Picazo, A., Peštová, D., Reyes, F.B., Hernández, J.R.M., Alcocer, J., Ibarra, M.M.,  
1248 Camacho, A.: Spirostomum teres: A Long Term Study of an Anoxic-Hypolimnion Population Feeding upon  
1249 Photosynthesizing Microorganisms. *Acta Protozool.* 59, 13–38.  
1250 <https://doi.org/10.4467/16890027AP.20.002.12158>, 2020.
- 1251 Marañón, E., Cermeño, P., Fernández, E., Rodríguez, J., Zabala, L.: Significance and mechanisms of  
1252 photosynthetic production of dissolved organic carbon in a coastal eutrophic ecosystem. *Limnol. Oceanogr.* 49,  
1253 1652–1666. <https://doi.org/10.4319/lo.2004.49.5.1652>, 2004.
- 1254 Margolin, A.R., Gerringa, L.J., Hansell, D.A. and Rijkenberg, M.J.: Net removal of dissolved organic carbon in  
1255 the anoxic waters of the Black Sea. *Marine Chemistry*, 183, pp.13–24.  
1256 <https://doi.org/10.1016/j.marchem.2016.05.003>, 2016.
- 1257 Mason, E., Edmonds, M., Turchyn, A.V.: Remobilization of crustal carbon may dominate volcanic arc  
1258 emissions. *Science* 357, 290–294. <https://doi.org/10.1126/science.aan5049>, 2017.
- 1259 Mercedes-Martín, R., Ayora, C., Tritlla, J., Sánchez-Román, M.: The hydrochemical evolution of alkaline  
1260 volcanic lakes: a model to understand the South Atlantic Pre-salt mineral assemblages. *Earth-Sci. Rev.* 198,  
1261 102938. <https://doi.org/10.1016/j.earscirev.2019.102938>, 2019.
- 1262 Milesi, V.P., Debure, M., Marty, N.C.M., Capano, M., Jézéquel, D., Steefel, C., Rouchon, V., Albéric, P., Bard,  
1263 E., Sarazin, G., Guyot, F., Virgone, A., Gaucher, É.C., Ader, M.: Early Diagenesis of Lacustrine Carbonates in  
1264 Volcanic Settings: The Role of Magmatic  $\text{CO}_2$  (Lake Dziani Dzaha, Mayotte, Indian Ocean). *ACS Earth Space*  
1265 *Chem.* 4, 363–378. <https://doi.org/10.1021/acsearthspacechem.9b00279>, 2020.



- 1266 Mook, W.G., Bommerson, J.C., Staverman, W.H.: Carbon isotope fractionation between dissolved bicarbonate  
1267 and gaseous carbon dioxide. *Earth Planet. Sci. Lett.* 22, 169–176. [https://doi.org/10.1016/0012-821X\(74\)90078-](https://doi.org/10.1016/0012-821X(74)90078-8)  
1268 [8](https://doi.org/10.1016/0012-821X(74)90078-8), 1974.
- 1269 Morana, C., Sarmiento, H., Descy, J.-P., Gasol, J.M., Borges, A.V., Bouillon, S., Darchambeau, F.: Production of  
1270 dissolved organic matter by phytoplankton and its uptake by heterotrophic prokaryotes in large tropical lakes.  
1271 *Limnol. Oceanogr.* 59, 1364–1375. <https://doi.org/10.4319/lo.2014.59.4.1364>, 2014.
- 1272 Núñez Useche, F., Barragán, R., Moreno Bedmar, J.A., Canet, C.: Mexican archives for the major Cretaceous  
1273 Oceanic Anoxic Events. *Bol. Soc. Geológica Mex.* 66, 491–505. <https://doi.org/10.18268/BSGM2014v66n3a7>,  
1274 2014.
- 1275 Ogawa, H., Amagai, Y., Koike, I., Kaiser, K., Benner, R.: Production of Refractory Dissolved Organic Matter by  
1276 Bacteria. *Science* 292, 917–920. <https://doi.org/10.1126/science.1057627>, 2001.
- 1277 O’Leary, M.H.: Carbon Isotopes in Photosynthesis. *BioScience* 38, 328–336. <https://doi.org/10.2307/1310735>,  
1278 1988.
- 1279 Paneth, P., O’Leary, M.H.: Carbon isotope effect on dehydration of bicarbonate ion catalyzed by carbonic  
1280 anhydrase. *Biochemistry* 24, 5143–5147. <https://doi.org/10.1021/bi00340a028>, 1985.
- 1281 Pardue, J.W., Scalán, R.S., Van Baalen, C., Parker, P.L.: Maximum carbon isotope fractionation in  
1282 photosynthesis by blue-green algae and a green alga. *Geochim. Cosmochim. Acta* 40, 309–312.  
1283 [https://doi.org/10.1016/0016-7037\(76\)90208-8](https://doi.org/10.1016/0016-7037(76)90208-8), 1976.
- 1284 Pecoraino, G., D’Alessandro, W., Inguaggiato, S.: The Other Side of the Coin: Geochemistry of Alkaline Lakes  
1285 in Volcanic Areas. In *Volcanic Lakes, Advances in Volcanology*. Springer, Berlin, Heidelberg, pp. 219–237.  
1286 [https://doi.org/10.1007/978-3-642-36833-2\\_9](https://doi.org/10.1007/978-3-642-36833-2_9), 2015.
- 1287 Petrash, D.A., Steenbergen, I.M., Valero, A., Meador, T.B., Pačes, T., Thomazo, C.: Aqueous system-level  
1288 processes and prokaryote assemblages in the ferruginous and sulfate-rich bottom waters of a post-mining lake.  
1289 *Biogeosciences* 19, 1723–1751. <https://doi.org/10.5194/bg-19-1723-2022>, 2022.
- 1290 Pimenov, N.V., Lunina, O.N., Prusakova, T.S., Rusanov, I.I., Ivanov, M.V.: Biological fractionation of stable  
1291 carbon isotopes at the aerobic/anaerobic water interface of meromictic water bodies. *Microbiology* 77, 751–759.  
1292 <https://doi.org/10.1134/S0026261708060131>, 2008.
- 1293 Posth, N.R., Bristow, L.A., Cox, R.P., Habicht, K.S., Danza, F., Tonolla, M., Frigaard, N. - U., Canfield, D.E.:  
1294 Carbon isotope fractionation by anoxygenic phototrophic bacteria in euxinic Lake Cadagno. *Geobiology* 15,  
1295 798–816. <https://doi.org/10.1111/gbi.12254>, 2017.
- 1296 Rendon-Lopez, M.J.: *Limnología física del lago crater los Espinos, Municipio de Jiménez Michoacan*. 2008.
- 1297 Ridgwell, A. and Arndt, S.: Why dissolved organics matter: DOC in ancient oceans and past climate change. In  
1298 *Biogeochemistry of marine dissolved organic matter* (pp. 1-20). Academic Press. [https://doi.org/10.1016/B978-](https://doi.org/10.1016/B978-0-12-405940-5.00001-7)  
1299 [0-12-405940-5.00001-7](https://doi.org/10.1016/B978-0-12-405940-5.00001-7), 2015.
- 1300 Riebesell, U., Burkhardt, S., Dauelsberg, A., Kroon, B.: Carbon isotope fractionation by a marine  
1301 diatom: dependence on the growth-rate-limiting resource. *Mar. Ecol. Prog. Ser.* 193, 295–303.  
1302 <https://doi.org/10.3354/meps193295>, 2000.
- 1303 Rothman, D.H., Hayes, J.M., Summons, R.E.: Dynamics of the Neoproterozoic carbon cycle. *Proc. Natl. Acad.*  
1304 *Sci.* 100, 8124–8129. <https://doi.org/10.1073/pnas.0832439100>, 2003.
- 1305 Sackett, W.M., Eckelmann, W.R., Bender, M.L., Bé, A.W.H.: Temperature Dependence of Carbon Isotope  
1306 Composition in Marine Plankton and Sediments. *Science* 148, 235–237.  
1307 <https://doi.org/10.1126/science.148.3667.235>, 1965.
- 1308 Saghai, A., Zivanovic, Y., Moreira, D., Benzerara, K., Bertolino, P., Ragon, M., Tavera, R., López- Archilla,  
1309 A.I. and López- García, P.: Comparative metagenomics unveils functions and genome features of microbialite-  
1310 associated communities along a depth gradient. *Environmental microbiology*, 18, 4990-5004.  
1311 <https://doi.org/10.1111/1462-2920.13456>, 2016.



- 1312 Saini, J.S., Hassler, C., Cable, R.N., Fourquez, M., Danza, F., Roman, S., Tonolla, M., Storelli, N., Jacquet, S.,  
1313 Zdobnov, E.M. and Duhaime, M.B.: Bacterial, phytoplankton, and viral dynamics of meromictic Lake Cadagno  
1314 offer insights into the Proterozoic ocean microbial loop. bioRxiv. <https://doi.org/10.1101/2021.10.13.464336>,  
1315 2021.
- 1316 Satkoski, A.M., Beukes, N.J., Li, W., Beard, B.L., Johnson, C.M.: A redox-stratified ocean 3.2 billion years ago.  
1317 Earth Planet. Sci. Lett. 430, 43–53. <https://doi.org/10.1016/j.epsl.2015.08.007>, 2015.
- 1318 Schidlowski, M.: Carbon isotopes as biogeochemical recorders of life over 3.8 Ga of Earth history: evolution of  
1319 a concept. Precambrian Res. 106, 117–134. [https://doi.org/10.1016/S0301-9268\(00\)00128-5](https://doi.org/10.1016/S0301-9268(00)00128-5), 2001.
- 1320 Schiff, S.L., Tsuji, J.M., Wu, L., Venkiteswaran, J.J., Molot, L.A., Elgood, R.J., Paterson, M.J., Neufeld, J.D.:  
1321 Millions of Boreal Shield Lakes can be used to Probe Archaean Ocean Biogeochemistry. Sci. Rep. 7, 46708.  
1322 <https://doi.org/10.1038/srep46708>, 2017.
- 1323 Sexton, P.F., Norris, R.D., Wilson, P.A., Pälike, H., Westerhold, T., Röhl, U., Bolton, C.T., Gibbs, S.: Eocene  
1324 global warming events driven by ventilation of oceanic dissolved organic carbon. Nature 471, 349–352.  
1325 <https://doi.org/10.1038/nature09826>, 2011.
- 1326 Shi, W., Li, C. and Algeo, T.J.: Quantitative model evaluation of organic carbon oxidation hypotheses for the  
1327 Ediacaran Shuram carbon isotopic excursion. Science China Earth Sciences, 60, 2118–2127.  
1328 <https://doi.org/10.1007/s11430-017-9137-1>, 2017.
- 1329 Siebe, C., Guilbaud, M.-N., Salinas, S., Chédeville-Monzo, C.: Eruption of Alberca de los Espinos tuff cone  
1330 causes transgression of Zacapu lake ca. 25,000 yr BP in Michoacán, México. Presented at the IAS 4IMC  
1331 Conference, Auckland, New Zeland, pp. 74–75. 2012.
- 1332 Siebe, C., Guilbaud, M.-N., Salinas, S., Kshirsagar, P., Chevrel, M.O., Jiménez, A.H., Godínez, L.: Monogenetic  
1333 volcanism of the Michoacán-Guanajuato Volcanic Field: Maar craters of the Zacapu basin and domes, shields,  
1334 and scoria cones of the Tarascan highlands (Paracho-Paricutin region). Presented at the Pre-meeting field guide  
1335 for the 5th international Maar Conference, Querétaro, México, pp. 1–37. 2014.
- 1336 Sigala, I., Caballero, M., Correa-Metrio, A., Lozano-García, S., Vázquez, G., Pérez, L., Zawisza, E.: Basic  
1337 limnology of 30 continental waterbodies of the Transmexican Volcanic Belt across climatic and environmental  
1338 gradients. Bol. Soc. Geológica Mex. 69, 313–370. <https://doi.org/10.18268/BSGM2017v69n2a3>, 2017.
- 1339 Silva Aguilera, R.A.: Analisis del descenso del nivel de agua del lago Alchichica, Puebla, México 120. 2019.
- 1340 Sirevag, R., Buchanan, B.B., Berry, J.A., Troughton, J.H.: Mechanisms of CO<sub>2</sub> Fixation in Bacterial  
1341 Photosynthesis Studied by the Carbon Isotope Fractionation Technique. Arch Microbiol 112, 35–38.  
1342 <https://doi.org/10.1007/BF00446651>, 1977.
- 1343 Soetaert, K., Hofmann, A.F., Middelburg, J.J., Meysman, F.J.R., Greenwood, J.: The effect of biogeochemical  
1344 processes on pH. Mar. Chem. 105, 30–51. <https://doi.org/10.1016/j.marchem.2006.12.012>, 2007.
- 1345 Swanson-Hysell, N.L., Rose, C.V., Calmet, C.C., Halverson, G.P., Hurtgen, M.T. and Maloof, A.C.: Cryogenian  
1346 glaciation and the onset of carbon-isotope decoupling. Science, 328, 608–611. DOI: [10.1126/science.1184508](https://doi.org/10.1126/science.1184508),  
1347 2010.
- 1348 Talbot, M.R.: A review of the palaeohydrological interpretation of carbon and oxygen isotopic ratios in primary  
1349 lacustrine carbonates. Chem. Geol. Isot. Geosci. Sect. 80, 261–279. [https://doi.org/10.1016/0168-9622\(90\)90009-2](https://doi.org/10.1016/0168-9622(90)90009-2),  
1350 1990.
- 1351 Thomas, P.J., Boller, A.J., Satagopan, S., Tabita, F.R., Cavanaugh, C.M., Scott, K.M.: Isotope discrimination by  
1352 form IC RubisCO from *Ralstonia eutropha* and *Rhodobacter sphaeroides*, metabolically versatile members of ‘  
1353 *Proteobacteria*’ from aquatic and soil habitats. Environ. Microbiol. 21, 72–80. <https://doi.org/10.1111/1462-2920.14423>,  
1354 2019.
- 1355 Thornton, D.C.O.: Dissolved organic matter (DOM) release by phytoplankton in the contemporary and future  
1356 ocean. Eur. J. Phycol. 49, 20–46. <https://doi.org/10.1080/09670262.2013.875596>, 2014.



- 1357 Tziperman, E., Halevy, I., Johnston, D.T., Knoll, A.H. and Schrag, D.P.: Biologically induced initiation of  
1358 Neoproterozoic snowball-Earth events. *PNAS*, 108, 15091-15096.  
1359 [www.pnas.org/cgi/doi/10.1073/pnas.1016361108](http://www.pnas.org/cgi/doi/10.1073/pnas.1016361108), 2011.
- 1360 Ussiri, D.A.N., Lal, R.: Carbon Sequestration for Climate Change Mitigation and Adaptation. Springer  
1361 International Publishing, Cham. <https://doi.org/10.1007/978-3-319-53845-7>, 2017.
- 1362 van Mooy, B.A.S., Keil, R.G., Devol, A.H.: Impact of suboxia on sinking particulate organic carbon: Enhanced  
1363 carbon flux and preferential degradation of amino acids via denitrification. *Geochim. Cosmochim. Acta* 66, 457–  
1364 465. [https://doi.org/10.1016/S0016-7037\(01\)00787-6](https://doi.org/10.1016/S0016-7037(01)00787-6), 2002.
- 1365 Vilaclara, G., Chávez, M., Lugo, A., González, H., Gaytán, M.: Comparative description of crater-lakes basic  
1366 chemistry in Puebla State, Mexico. *SIL Proc.* 1922-2010 25, 435–440.  
1367 <https://doi.org/10.1080/03680770.1992.11900158>, 1993.
- 1368 van Vliet, D.M., Meijerfeldt, F.A.B., Dutilh, B.E., Villanueva, L., Sinnighe Damsté, J.S., Stams, A.J.M.,  
1369 Sánchez- Andrea, I.: The bacterial sulfur cycle in expanding dysoxic and euxinic marine waters. *Environ.*  
1370 *Microbiol.* 23, 2834–2857. <https://doi.org/10.1111/1462-2920.15265>, 2021.
- 1371 Wang, S., Yeager, K.M., Lu, W.: Carbon isotope fractionation in phytoplankton as a potential proxy for pH  
1372 rather than for [CO<sub>2(aq)</sub>]: Observations from a carbonate lake. *Limnol. Oceanogr.* 61, 1259–1270.  
1373 <https://doi.org/10.1002/lno.10289>, 2016.
- 1374 Werne, J.P., Hollander, D.J.: Balancing supply and demand: controls on carbon isotope fractionation in the  
1375 Cariaco Basin (Venezuela) Younger Dryas to present. *Mar. Chem.* 92, 275–293.  
1376 <https://doi.org/10.1016/j.marchem.2004.06.031>, 2004.
- 1377 Wetz, M.S., Wheeler, P.A.: Release of dissolved organic matter by coastal diatoms. *Limnol. Oceanogr.* 52, 798–  
1378 807. <https://doi.org/10.4319/lo.2007.52.2.0798>, 2007.
- 1379 Whiticar, M.J., Faber, E., Schoell, M.: Biogenic methane formation in marine and freshwater environments: CO<sub>2</sub>  
1380 reduction vs. acetate fermentation—Isotope evidence. *Geochim. Cosmochim. Acta* 50, 693–709.  
1381 [https://doi.org/10.1016/0016-7037\(86\)90346-7](https://doi.org/10.1016/0016-7037(86)90346-7), 1986.
- 1382 Williams, P.M., Gordon, L.I.: Carbon-13: carbon-12 ratios in dissolved and particulate organic matter in the sea.  
1383 *Deep Sea Res. Oceanogr. Abstr.* 17, 19–27. [https://doi.org/10.1016/0011-7471\(70\)90085-9](https://doi.org/10.1016/0011-7471(70)90085-9), 1970.
- 1384 Wittkop, C., Teranes, J., Lubenow, B., Dean, W.E.: Carbon- and oxygen-stable isotopic signatures of  
1385 methanogenesis, temperature, and water column stratification in Holocene siderite varves. *Chem. Geol.* 389,  
1386 153–166. <https://doi.org/10.1016/j.chemgeo.2014.09.016>, 2014.
- 1387 Zeyen, N., Benzerara, K., Beysac, O., Daval, D., Muller, E., Thomazo, C., Tavera, R., López-García, P.,  
1388 Moreira, D., Duprat, E.: Integrative analysis of the mineralogical and chemical composition of modern  
1389 microbialites from ten Mexican lakes: What do we learn about their formation? *Geochim. Cosmochim. Acta*  
1390 305, 148–184. <https://doi.org/10.1016/j.gca.2021.04.030>, 2021.
- 1391 Zohary, T., Erez, J., Gophen, M., Berman-Frank, I., Stiller, M.: Seasonality of stable carbon isotopes within the  
1392 pelagic food web of Lake Kinneret. *Limnol. Oceanogr.* 39, 1030–1043.  
1393 <https://doi.org/10.4319/lo.1994.39.5.1030>, 1994.
- 1394 Zyakun, A.M., Lunina, O.N., Prusakova, T.S., Pimenov, N.V., Ivanov, M.V.: Fractionation of stable carbon  
1395 isotopes by photoautotrophically growing anoxygenic purple and green sulfur bacteria. *Microbiology* 78, 757–  
1396 768. <https://doi.org/10.1134/S0026261709060137>, 2009.